Application of air injectors to biomass combustion systems. Conveyance of rice husks and other particulate biomass materials (NRI Bulletin 52)

Natural Resources Institute

Bulletin 52

APPLICATION OF AIR INJECTORS TO BIOMASS COMBUSTION SYSTEMS

Conveyance of rice husks and other particulate biomass materials

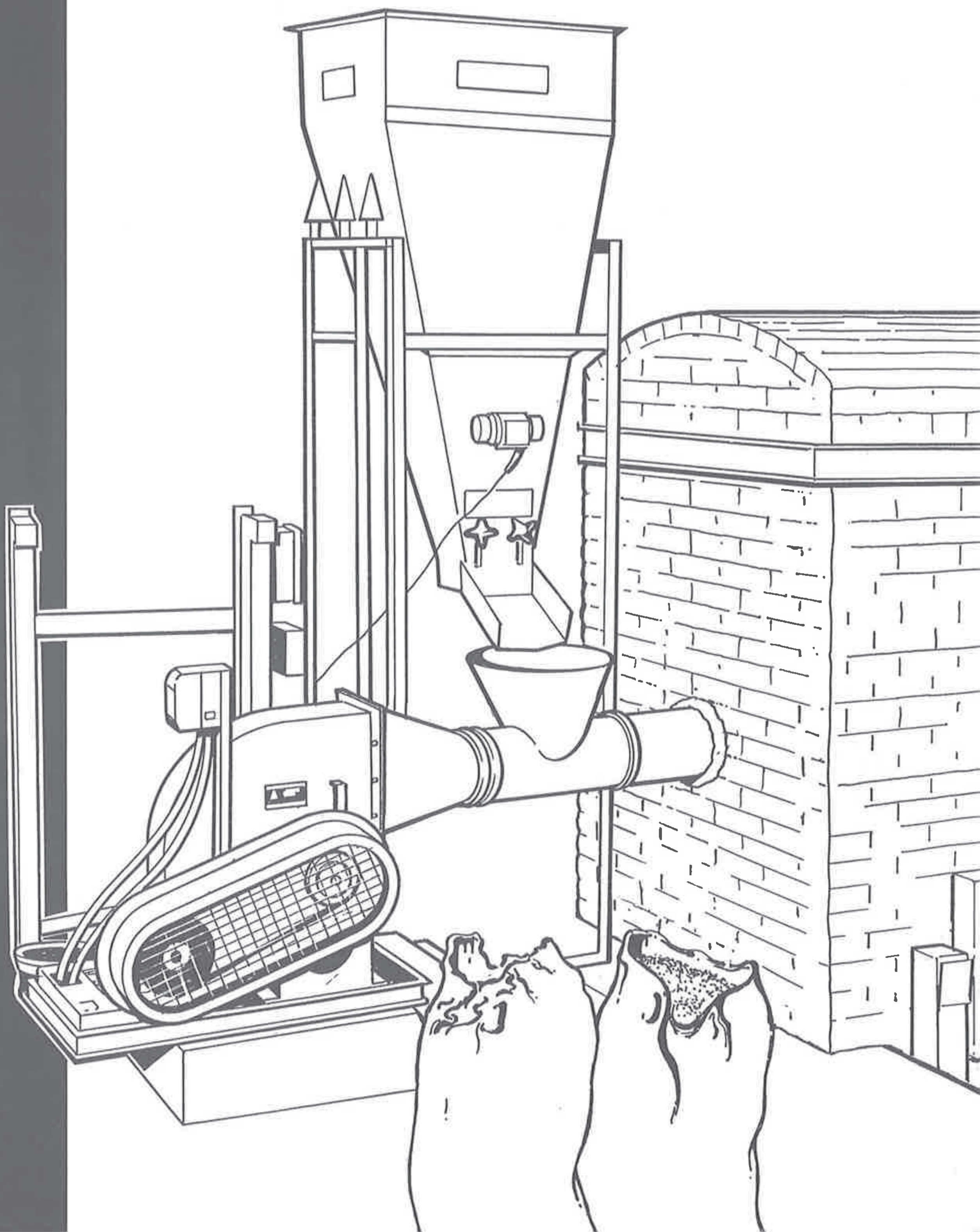

Overseas Development Administration

APPLICATION OF AIR INJECTORS TO BIOMASS COMBUSTION SYSTEMS

Conveyance of rice husks and other particulate biomass materials

A. S. Tariq and R. J. Lipscombe

Bulletin 52

Natural Resources Institute

The scientific arm of the
Overseas Development Administration

The Natural Resources Institute (NRI) is an internationally recognized centre of expertise on the natural resources sector in developing countries. It forms an integral part of the British Government's overseas aid programme. Its principal aim is to alleviate poverty and hardship in developing countries by increasing the productivity of their renewable natural resources. NRI's main fields of expertise are resource assessment and farming systems, integrated pest management, food science and crop utilization.

NRI carries out research and surveys; develops pilot-scale plant, machinery and processes; identifies, prepares, manages and executes projects; provides advice and training; and publishes scientific and development material.

Price £7.50

No charge is made for single copies of this publication sent to governmental and educational establishments, research institutions and non-profit-making organizations working in countries eligible for British Government Aid. Free copies cannot normally be addressed to individuals by name but only under their official titles.

Natural Resources Institute
ISBN 0 85954 307-2
ISSN 0952 8245

Contents

Appendices

ACKNOWLEDGEMENTS

The authors acknowledge the support and advice of colleagues, especially: Dr D. A. V. Dendy, Mr G. R. Breag and Mr A. P. Robinson for their encouragement and advice; Mr P. Reupke for his useful comments in the preparation of the draft; Mr A. J. Hawkes and Mr G. Anstee for the production of the figures; Mr I. Husson for his valuable assistance during the experimental work. Support from the Natural Resources Institute's Cereals and Pulses Food Security programme is gratefully acknowledged.

Summaries

SUMMARY

This bulletin describes work carried out by the Process and Storage Engineering Department of the Natural Resources Institute on the conveyance of particulate biomass materials by means of low-pressure air injectors for applications in small-scale to medium-scale combustion systems. Experimental data on the injector entrainment ratios for particulate-laden gases are compared with values calculated from theory. Procedures are given for an injector design optimized for minimum fan-power and fan-pressure requirements. It is concluded that the theoretical procedures developed for injector design and performance prediction for clean gases can also be applied, with simple modifications, to the dilute-phase entrainment of particulate materials in the injectors. This publication is primarily intended for use by engineers in the design of injector systems for application in small-scale to medium-scale particulate biomass combustion systems.

RESUME

Le présent bulletin décrit les travaux exécutés par le Département d'ingénierie de processus et d'entreposage du Natural Resources Institute (Institut des ressources naturelles) en ce qui concerne le transport des matières biomasses macroparticules grâces à des injecteurs d'air basse pression destinées à des applications dans des systèmes de combustion de petite à moyenne échelle. Les données expérimentales concernant les rapports d'entrainement des injecteurs pour les gaz chargés de macroparticules sont comparées aux valeurs calculées sur une base théorique. Il est fourni des procédures pour l'étude d'injecteurs optimisés conformément aux exigences minimum de puissance et de pression de ventilateur. Il est conclu que les procédures théoriques mises au point pour létude des injecteurs et les prévisions des performances pour des gaz épurés peuvent également être appliquées, avec des modifications simples, à l'entrainement en phase diluée des macroparticules dans les injecteurs. Cette pubication est principalement destinée aux ingénieurs pour l'étude des systèmes d'injecteurs pour application dans les systèmes de combustion de biomasses macroparticules à petite et moyenne échelle.

RESUMEN

En este boletin se describe la labor llevada a cabo por el Departamento Técnico de Almacenamiento y Procesos del Instituto de Recursos Naturales sobre el transporte de biomasa particulada por medio de inyectores neumáticos de baja presión, para aplicación en sistemas de combustión de pequeña a mediana escala. También se lleva a cobo la comparación de datos experimentales sobre las relaciones de arrastre del inyector para gases cargados con materiales particulados con valores calculados a partir de datos teóricos. Además, se presentan procedimientoos de diseño del inyector, optimizados para requisitos mínimos de presión y potencia del ventilador. el estudio concluye que los procedimientos teóricos desarrollados para el diseño del inyector y predicción del rendimiento para gases limpios puede tener asimismo aplicación, mediante la introducción de sencillas modificaciones, al arrastre en fase diluida de materiales particulados en los inyectores. Dirigida fundamentalmente a ingenieros, esta publicación será de utilidad en el diseño de sistemas de inyección para aplicación en sistemas de combustión de biomasa particulada de pequeña a mediana escala.

Section 1

Introduction

BACKGROUND

In developing countries considerable quantities of forestry and agricultural residues are generated in small-scale to medium-scale industrial processing centres such as those for rice, wood and oilseeds. Based upon the production data for rice and logs for sawnwood (FAO, 1989; 1990), it is estimated that approximately 108 million tonnes of rice husk and 87 million tonnes of sawdust are generated world-wide. A significant proportion of these residues could be economically exploited, for example 20% of the total rice-husk production offers full opportunity for beneficial development (Beagle, 1978). Although these residues are a potential source of energy, they are often treated by the industries concerned as waste materials and present disposal problems. In many instances industries which generate these residues have a requirement for process heat and motive power: this energy demand is met by either fuelwood or fossil fuels. The residues could however be used to meet either all or part of this energy requirement if equipment of the correct size, cost and performance is developed for their efficient conversion to energy.

Efficient conversion of these residues to energy offers many benefits in that it could: reduce pressure on dwindling fuelwood resources; reduce pollution from combustion of fossil fuels; generate revenue through import substitution; and provide opportunities for establishing local processing and manufacturing industries. Use of these residues for energy, instead of uncontrolled dumping, will alleviate local environmental problems.

DEVELOPMENT OF THE SYSTEM

With these benefits in mind, the Natural Resources Institute (NRI) has been developing combustion systems to burn particulate biomass residues efficiently for process heat and motive power applications in developing countries (Robinson, 1991; Robinson *et al.*, 1992; Robinson and Breag, 1992). This publication is part of an ongoing programme of work to maximize sustainable and beneficial utilization of agricultural and forestry residues for energy.

In the past NRI has used rotary and vibratory table feeders for particulate biomass suspension burner systems for energy production in small-scale to medium-scale industries. In these combustion systems, the particulate material was sucked into a stream of air and blown to the burner via a combustion-air fan. The system proved to be simple and adequate for many applications. However rice husks, an abrasive material, caused rapid erosion of the fan blades and fan housing. For example, when the system was used with rice husks as fuel at a rice mill in Sri Lanka – employing the NRI suspension burner – new fan blades were required in six weeks.

In view of the above difficulty, experimental and related theoretical work was undertaken at NRI to develop a particulate conveyance system using the well-established principle of a low-pressure air injector. Injectors, ejectors and jet pumps belong to a family of devices in which the momentum of a jet is used to entrain a secondary fluid. Such devices have been used in many applications, for example, movement of gases at high temperatures, exhausting fumes, vacuum evaporation, distillation, and atmospheric aerated gas burners (Kroll, 1947; Thring, 1962; Pritchard *et al.*, 1977; Francis, 1956).

The performance of an injector, designed for experimental flexibility and an extended range of experimental conditions, was evaluated at NRI for the entrainment of dust-laden gases to simulate conveyance of rice husks and sawdust. The primary aim of this work was to obtain experimental verification of the theoretical procedures in order to define design criteria for these systems. The experimental work was carried out using sawdust for convenience, but the results obtained are applicable to a range of small particulate biomass materials including rice husks. Sawdust mass flow-rates were varied between 40 and 190 kg/h for total air mass flow-rates of between 400 and 1700 kg/h. Back pressure on the injector was varied from 0 to 1800 N/m^2 (gauge). The latter pressure was not exceeded because back pressures above this value would not normally be expected in furnace/heat exchanger designs used in the agricultural and forestry industries envisaged.

SCOPE OF BULLETIN

In this bulletin the theory of low-pressure air injectors is given in detail in Section 2 and in Section 3 the experimental procedures and results obtained are described and compared with the theory. Good agreement between the theory and experiment was found for the solids-to-air mass ratios likely to be encountered for the applications of injectors to small-scale to medium-scale particulate biomass combustion systems in developing countries. In Section 4, a methodology for the design of injector systems for application in small-scale to medium-scale particulate biomass combustion systems is developed. This is based on the theory given in Section 2, the findings in Section 3 and NRI's experience in the combustion field. The procedures are explained with the help of an example calculation and lead to a design optimized for minimum fan-power and fan-pressure requirements. Figure 1 shows an injector designed, installed and operated by NRI – based on the work carried out in the UK – at a commercial rice mill in Sri Lanka.

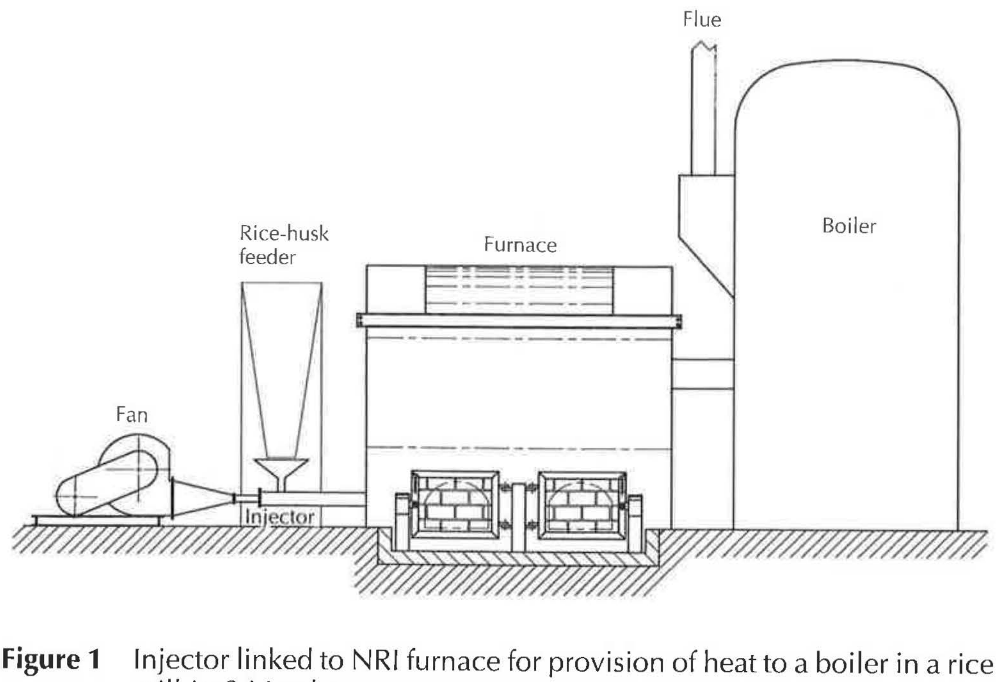

Figure 1 Injector linked to NRI furnace for provision of heat to a boiler in a rice mill in Sri Lanka

Section 2

Principles of low-pressure air injector systems

In this section the theory developed for clean gases (Francis, 1964), is applied to the entrainment of particulate-laden gases in low-pressure injectors. This requires a method to calculate pressure drops for particulate-laden gases. Existing information on the pressure drops for pneumatic conveyance of particulates (Perry and Green, 1984; Geldart, 1986) is incomplete, for the present work, and its inclusion in the theory of injector performance renders the resulting equations cumbersome and difficult to solve. Therefore, assumptions have been made in order to calculate these pressure losses and a simpler mathematical model of the system has been developed for entrainment of particulate-laden gases with low solids-to-air ratios.

FREE JETS

When a fluid emerges from a nozzle it interacts with, and entrains, the surrounding fluid and consequently expands. The momentum from the jet is transferred to the surrounding fluid that is being entrained. A general description of a jet is given in Figure 2. Jet flows, in the fully developed region, exhibit similarity and their behaviour is described by simple non-dimensional correlations (Beer and Chigier, 1972; Perry and Green, 1984). The lengths of the potential core and transition region are approximately 5 and 10 nozzle diameters respectively and the jet angle is of the order of 20°. The entrainment rates for free jets are high and this is shown by the fact that, every three nozzle diameters distance along the axis, the quantity of fluid entrained is equal to the mass flowrate of fluid at the nozzle exit. This ability of free jets, to entrain copious quantities of the surrounding fluid is used in injectors and similar devices.

INJECTORS

Figure 3 depicts a typical injector arrangement and also shows the variables used in this section and their relation to various components of the injector. In many applications the diffuser shown in Figure 3 is omitted. In an injector the entraining jet fluid is accelerated through a nozzle, forming a high-velocity turbulent jet with which entrained fluid mixes. A large velocity gradient exists at

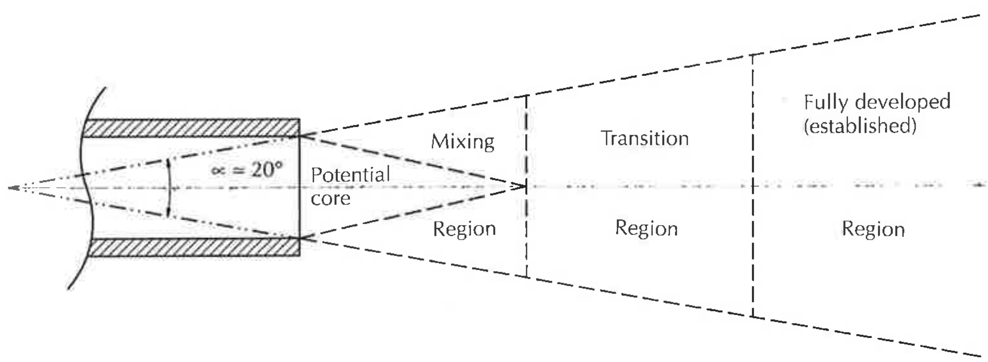

Figure 2 Regions of a free jet

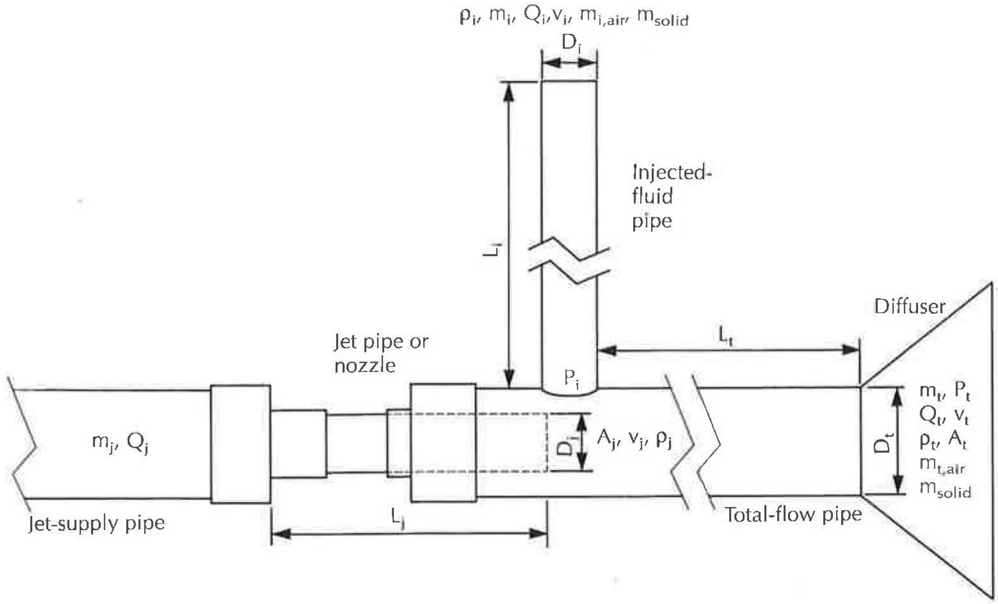

Figure 3 Typical injector and definition of variables

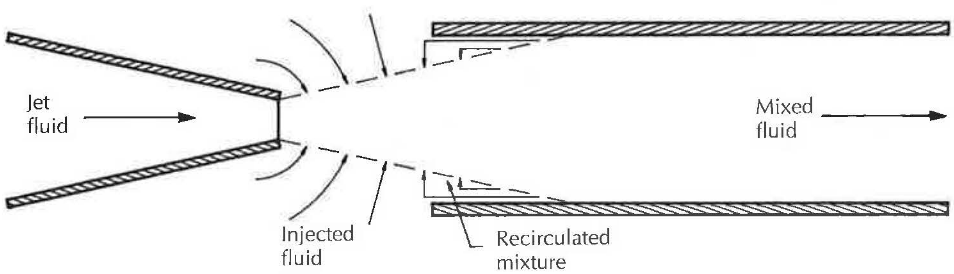

Figure 4 Approximate flow pattern at the total-flow pipe entrance

the edges of the jet as it emerges from the nozzle, and the resulting shearing action draws in the surrounding fluid and carries it forward to the total-flow pipe. Figure 4 shows the flow patterns at the entrance of the total-flow pipe. Mixing of the two streams occurs by eddy diffusion and during the initial mixing process momentum is conserved; the pressure is substantially constant and the jet spreads as a turbulent free jet. The jet of mixed fluid continues to expand to fill the total-flow pipe by entrainment of the recirculated fluid. Momentum is lost in this process and some recovery of static pressure occurs. The key to the calculation of the injector performance is the application of the force-momentum balance to the mixing process in the total-flow pipe, in order to find the rise in static pressure.

From the momentum theorem the following governing equation for the injector performance can be derived (Francis, 1964):

$$\left[(P_t - P_i) + S_{12}\frac{m_t Q_t}{2A_t^2}\right] A_t + \frac{m_t Q_t}{A_t} - \frac{m_j Q_j}{A_j C_j} = 0 \qquad (1)$$

where P_t is the back pressure (gauge) at the end of the total-flow pipe

P_i is the pressure (gauge) at the outlet of the injected-fluid pipe

Q_t and Q_j are the volumetric flow-rates of total fluid and jet fluid

m_t and m_j are the mass flow-rates of total fluid and jet fluid

A_t and A_j are the cross-sectional areas of the total-flow pipe and the jet pipe

C_j is the discharge coefficient for the jet nozzle and can be estimated from (Geldart, 1986):

$$C_j = 0.82 \left(\frac{L_j}{D_j}\right)^{0.13} \quad \text{for } L_j/D_j > 0.09$$

with the limit that $C_j = 1$ for $L_j \geq 4.6D_j$

and for conditions $D_j \gg L_j$, $C_j = 0.6$ (corresponds to an orifice in a thin plate)

L_j is the length of the parallel section of the jet-nozzle

S_{12} is the wall friction pressure-loss coefficient for the total-flow pipe. The pressure loss is given by the multiple of S_{12} and the velocity head of the fluid in the pipe. For the cylindrical pipe used in the present work S_{12} is given by:

$$S_{12} = \frac{4fL_t}{D_t} \tag{2}$$

where f is the Fanning friction factor and

D_t and L_t are the diameter and length of the total-flow pipe respectively.

Assumptions made for the derivation of Equation 1 are as follows (Francis, 1964):

1 Turbulent conditions prevail in the jet and at the end of the throat or the total-flow pipe, implying that velocity, composition and temperature are reasonably uniform over a cross-section at these two positions.

2 The injected fluid enters the mixing-section substantially at right-angles to the jet axis, and therefore contributes negligible axial momentum. This is never strictly true but is a good approximation in most cases, giving slightly conservative estimates of the injector performance.

3 No phase changes take place.

4 The flow between the nozzle exit and the diffuser exit is incompressible, i.e. the density changes due to absolute pressure changes are negligible. This does not rule out density changes due to change of temperature.

5 Buoyancy effects are unimportant.

A further assumption made during the present work for application of Equation 1 to particulate-laden gases is that the pressure losses in the injected-fluid pipe and total-flow pipe can be calculated from the effective densities of the fluids in these pipes and the viscosity of the clean air. In Appendix 1 it will be shown that for the solids-to-air ratios encountered during this work, the above assumption gives results which for practical design purposes are identical to a more detailed treatment. With this assumption, the pressure P_i at the outlet of the injected-fluid pipe is given by:

$$P_i = -T_{coeff} \times \frac{1}{2} \rho_i v_i^2 \tag{3}$$

where

$$T_{coeff} = \begin{pmatrix} \text{Wall} & & \text{Entrance} & & \text{Velocity} \\ \text{friction loss} & + & \text{loss} & + & \text{head} \\ \text{coefficient} & & \text{coefficient} & & \text{coefficient} \end{pmatrix} \tag{4}$$

The pressure-loss coefficient for the wall friction is given by $4fL/D$; the entrance pressure-loss coefficient was taken to be 0.5 for the entrance of fluid from a large reservoir to a square-edged pipe (Rose and Cooper, 1977); and the velocity-head coefficient is unity.

Substituting for P_i from Equation 3, $Q = m/\rho$, $v = m/\rho A$ and multiplying throughout by A_t, Equation 1 is written as:

$$P_tA_t^2 + \frac{1}{2}T_{\text{coeff}}\frac{1}{\rho_i}\left(\frac{A_t}{A_i}\right)^2 m_i^2 + S_{12}\frac{1}{2\rho_t}m_t^2 + \frac{1}{\rho_t}m_t^2 - \frac{1}{C_j\rho_j}\left(\frac{A_t}{A_j}\right)m_j^2 = 0 \quad (5)$$

Substituting for mass conservation $m_i = m_t - m_j$ in Equation 5 and rearranging gives:

$$\left[\frac{1}{2}T_{\text{coeff}}\frac{1}{\rho_i}\left(\frac{A_t}{A_i}\right)^2 - \frac{1}{C_j\rho_j}\left(\frac{A_t}{A_j}\right)\right]m_j^2 + \frac{1}{2}T_{\text{coeff}}\frac{1}{\rho_i}\left(\frac{A_t}{A_i}\right)^2(-2m_t\, mj) +$$
$$\left[\left\{\frac{1}{2}T_{\text{coeff}}\frac{1}{\rho_i}\left(\frac{A_t}{A_i}\right)^2 + \left(\frac{S_{12}}{2}+1\right)\frac{1}{\rho_t}\right\}m_t^2 + P_tA_t^2\right] = 0 \quad (6)$$

To simplify Equation 6, the following are defined:

$$\alpha = \frac{1}{2}T_{\text{coeff}}\frac{1}{\rho_i}\left(\frac{A_t}{A_i}\right)^2 \quad (7) \qquad \beta = \left(\frac{S_{12}}{2}+1\right)\frac{1}{\rho_t} \quad (8)$$

$$\gamma = \frac{1}{C_j\rho_j}\left(\frac{A_t}{A_j}\right) \quad (9) \qquad \theta = P_tA_t^2 \quad (10)$$

The effective densities ρ_i and ρ_t of the particulate-laden air in the injected-fluid pipe and total-flow pipe can be derived from:

$$\rho_i = \rho_j\left(1 + \frac{m_{\text{solid}}}{(m_{t,\text{air}} - m_j)}\right) \quad (11) \qquad \rho_t = \rho_j\left[1 + \frac{m_{\text{solid}}}{m_{t,\text{air}}}\right] \quad (12)$$

where ρ_j is the density of the jet air.

By substituting from Equations 7, 8, 9 and 10, Equation 6 can be written as:

$$(\alpha - \gamma)m_j^2 + \alpha(-2m_t)m_j + \left[(\alpha + \beta)m_t^2 + \theta\right] = 0 \quad (13)$$

This is a quadratic equation of the form:

$$am_j^2 + bm_j + c = 0 \quad (14)$$

where

$$a = (\alpha - \gamma),\ b = -2\alpha m_t \text{ and } c = \left[(\alpha + \beta)m_t^2 + \theta\right]$$

and the valid solution for m_j is given by:

$$m_j = \frac{-b + \sqrt{b^2 - 4ac}}{2a} \quad (15)$$

For a given total air mass flow-rate requirement and injector geometry, Equation 15 can be solved directly to give the jet mass flow-rate for solids-free conditions. For conditions when solids are present, Equation 15 cannot be directly solved as ρ_i in Equation 11 requires knowledge of the jet mass flow-rate (m_j). In this case an iterative procedure can be used where m_j is first calculated for clean air conditions. This value of m_j is subsequently used in Equation 11 to evaluate ρ_i. This new ρ_i is then used in Equation 15 to derive a better value of m_j. The procedure is repeated and in about five iterations a converged value of m_j can be derived.

The evaluation of S_{12} and T_{coeff} requires knowledge of the Fanning friction factors. These can be obtained from graphical representations or correlations in publications, standard books on fluid mechanics and engineering handbooks (Perry and Green, 1984; Coker, 1991). For this work Fanning friction factors were calculated from the Colebrook equation (Colebrook, 1939):

$$\frac{1}{f^{0.5}} = -4\log\left(\frac{\varepsilon}{3.7D} + \frac{1.256}{\text{Re}\, f^{0.5}}\right) \quad (16)$$

Solution of the above equation was obtained by the Newton-Raphson technique.

Expressing Equation 16 as function $F(f)$:

$$F(f) = f^{0.5} \exp\left(\frac{-1}{Gf^{0.5}}\right) - \frac{f^{0.5}}{3.7}\left(\frac{\varepsilon}{D}\right) - \frac{1.256}{Re} = 0 \tag{17}$$

the derivative $F'(f)$ of the function $F(f)$ is then given by:

$$F'(f) = 0.5f^{-0.5}\left[\exp\left(\frac{-1}{Gf^{0.5}}\right)\left(1 + \frac{f^{-0.5}}{G}\right) - \frac{0.5}{3.7}\left(\frac{\varepsilon}{D}\right)\right] \tag{18}$$

where G in Equation 17 and 18 results from conversion of the common logarithms to the natural logarithms and coefficient 4 in Equation 16; G is given by:

$$G = 4/\ln 10 = 1.7372$$

The solution for the Fanning friction factor for a given Reynolds number (Re) and relative pipe-roughness factor (ε/D) is then given by the following iterative method:

$$f_{k+1} = f_k - \left(\frac{F(f_k)}{F'(f_k)}\right) \tag{19}$$

where f_{k+1} is a better estimate than f_k, and a starting value of 0.035 for f_k results in a converged solution in a few iterations.

A BASIC computer program based on the foregoing is given in Appendix 4. This program calculates the jet flow-rate required and other injector performance parameters for a given injector geometry, solids mass flow-rate, total air mass flow-rate and back pressure at the injector outlet.

Section 3

Experimental work

MEASUREMENTS WITH CLEAN AIR

The injector shown in Figure 5 was used for the experimental investigations. A high-pressure blower provided air for an extended range of injector operation. Velocity measurements were made at locations at least 10 pipe-diameters axial distance from any flow disturbances. Initial measurements for clean air were made with a 2.3 mm diameter pitot-static tube in the jet-supply pipe, injected-fluid pipe and the total-flow pipe at the locations indicated in Figure 5. Two velocity profiles for each pipe were measured at mutually perpendicular axes. The measuring points on each axis, shown in Figure 6, were in accordance with the instructions supplied by the pitot-static tube manufacturer, Air Flow Developments Ltd. Except for the jet-supply pipe at very small flow-rates, the velocity profiles for all of the measurements showed fully developed turbulent flow with no significant asymmetries along the two measuring axes. Examples of the velocity profiles obtained for the three pipes are shown in Figure 7.

Since the air temperature increased through the high-pressure fan, air temperatures in each of the pipes were recorded at the pitot-static measuring points. From these measurements, mass flow-rates for each of the three pipes were calculated from:

$$V_{ave} = \left[\frac{2}{\rho}\left(\frac{\Sigma\Delta P}{20}\right)\right]^{0.5}$$

where ΔP is the differential pressure as measured by the pitot-static tube.

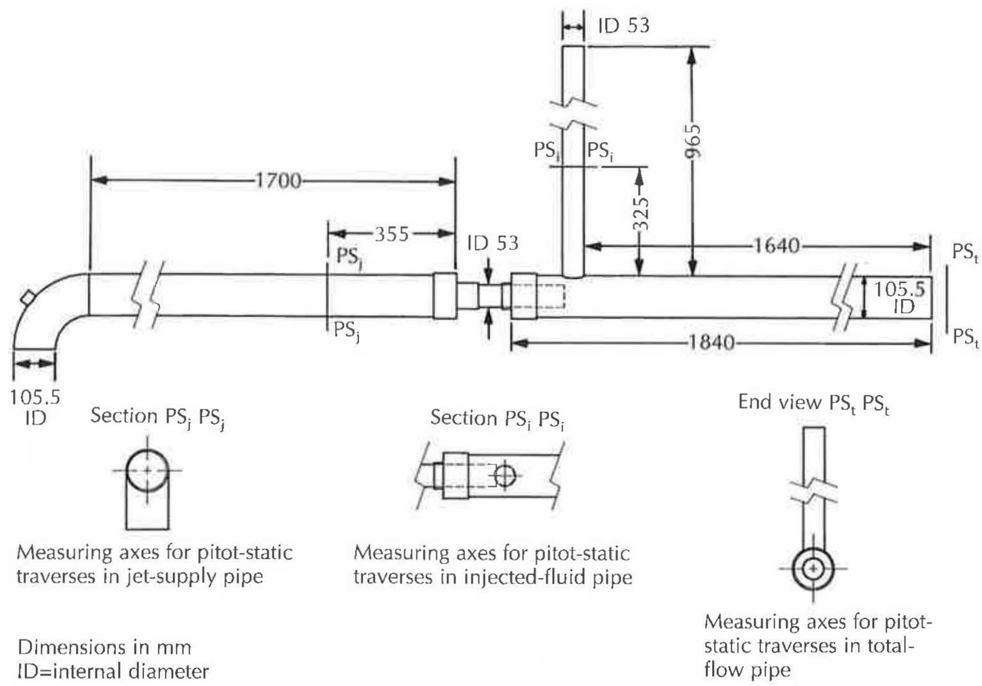

Figure 5 Injector used for experimental investigations

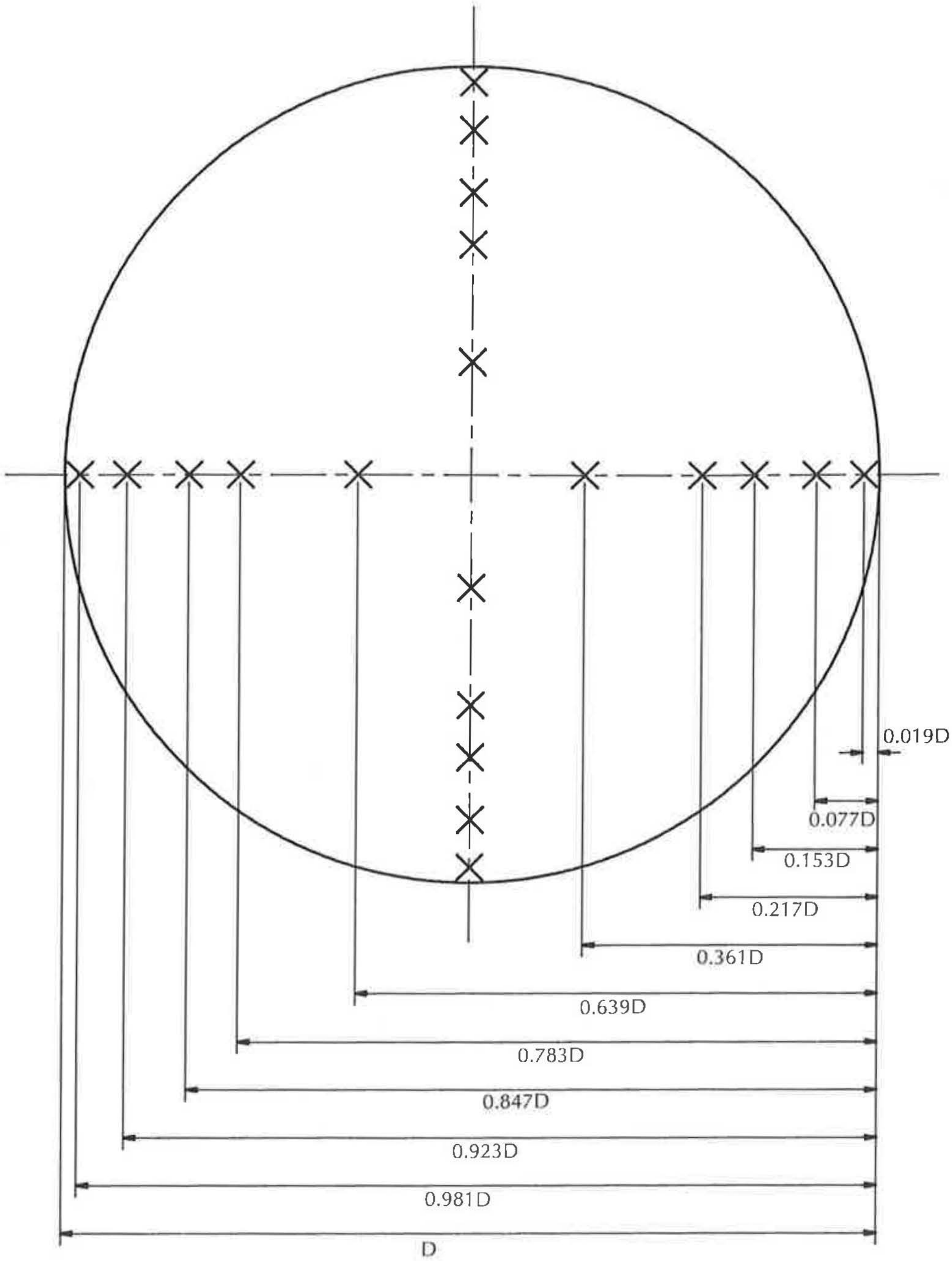

Figure 6 Pitot-static measuring points for velocity profiles (in accordance with manufacturers' instructions)

The mass flow-rate (m) in kg/h is then given by:

$$m = 3600\, A\, v_{ave}\, \rho$$

where ρ is the density and is calculated from the measured static pressures and temperatures.

To measure entrainment ratios with back pressure, a conical restrictor at the outlet of the total-flow pipe was used. This arrangement and the flow-measuring points for the total-flow pipe are shown in Figure 8. Velocity profiles measured in the total-flow pipe with a conical restrictor also exhibited fully developed turbulent-flow conditions. For some of the measurements with the conical restrictor in place, flow-rates in the jet-supply pipe were measured with an

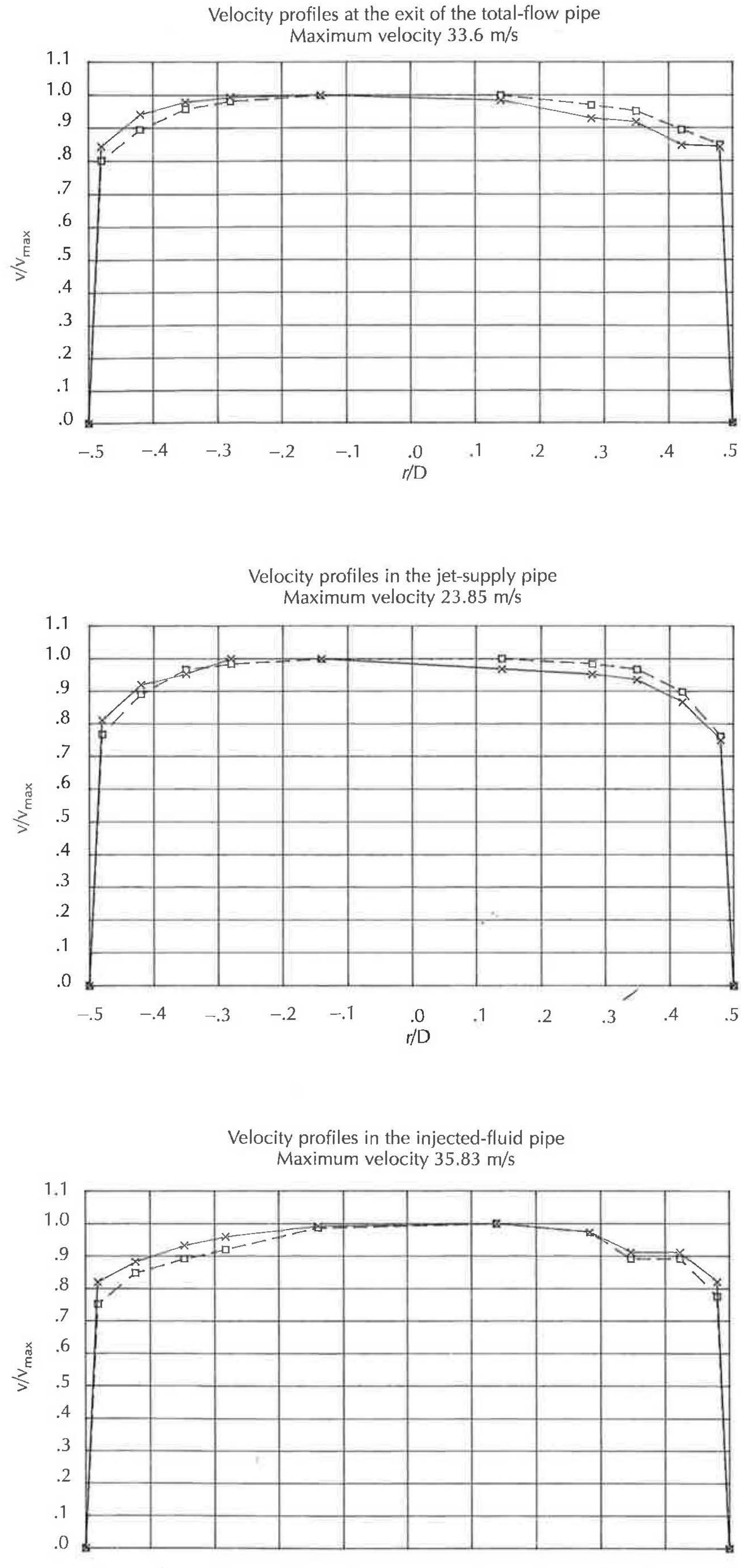

Figure 7 Velocity profiles for the total-flow pipe, jet-supply pipe and injected-fluid pipe at two mutually perpendicular axes

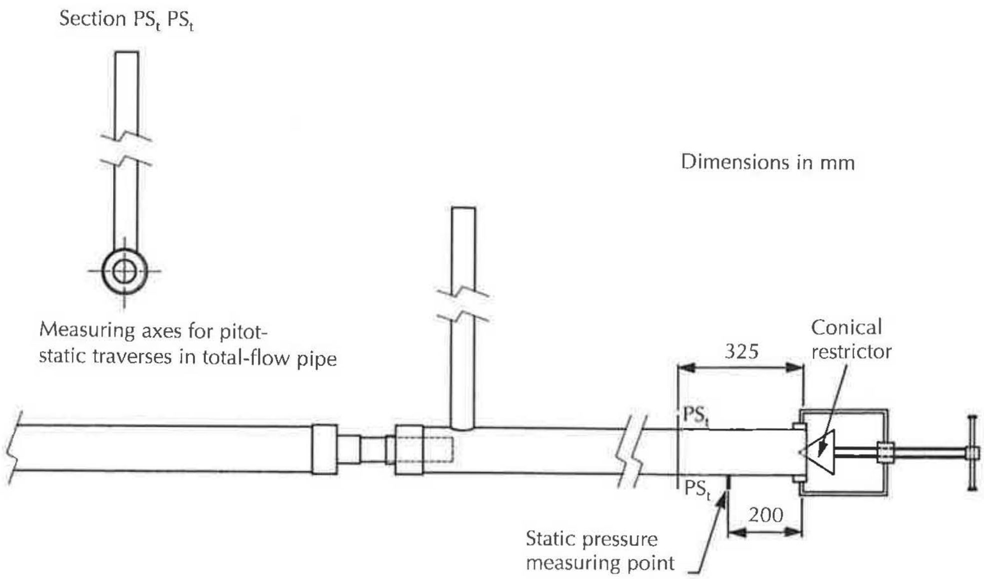

Figure 8 Arrangement for inducing back pressure on the injector

'Annubar' flow sensor. The Annubar used during this work is shown in Figure 9 and its installation in the jet-supply pipe is shown in Figure 10. The Annubar was calibrated *in situ* with pitot-static tube traverses. The details of this calibration are given in Appendix 2.

Accuracy of the mass-flow measurements for the injector (with both Annubar and pitot-static tube) is indicated by the mass balance for the three air streams:

$$m_{t,air} = m_j + m_{i,air} \tag{21}$$

The mass balance between $m_{t,air}$ and the sum of m_j and $m_{i,air}$ was found to be close, with an absolute average deviation of 1.6% for 35 data points. The percentage absolute deviation was calculated as:

$$\% \text{ deviation} = \left| \frac{m_{t,air} - (m_j + m_{i,air})}{m_{t,air}} \right| \times 100 \tag{22}$$

The entrainment ratio E for the injector is now defined as:

$$E = \frac{m_t}{m_j} \tag{23}$$

The experimentally determined entrainment ratios, at back pressures of 0, 250, 500, 1000 and 1550 N/m^2 (gauge) were compared against the values calculated in accordance with the procedures given in Section 2. The plots of the measured and calculated entrainment ratios against the total mass flow-rates are shown in Figure 11. Experimental and calculated values of the entrainment ratio were found to be closely correlated. The percentage difference between the two was calculated as below:

$$\% \text{ difference} = \frac{\begin{matrix}\text{Calculated} & \text{Measured}\\ \text{entrainment ratio} & - \text{ entrainment ratio}\end{matrix}}{\text{Calculated entrainment ratio}} \times 100 \tag{24}$$

The percentage difference showed no significant systematic trend, though at higher back pressures the measured values tended to be greater than the calculated values. However the differences were small and results for the calculated and the measured values are given in Table 1.

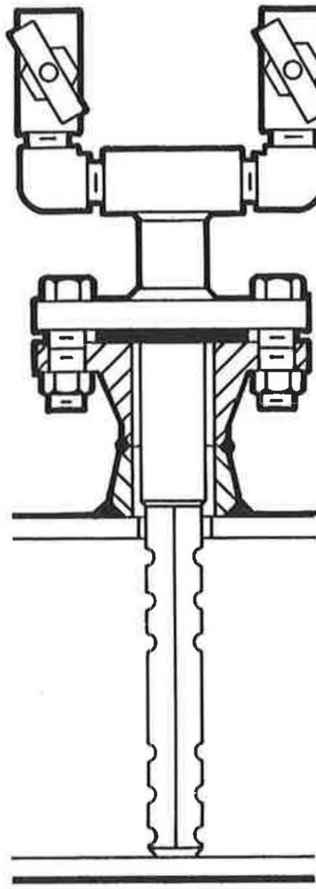

Figure 9 The Annubar flow sensor

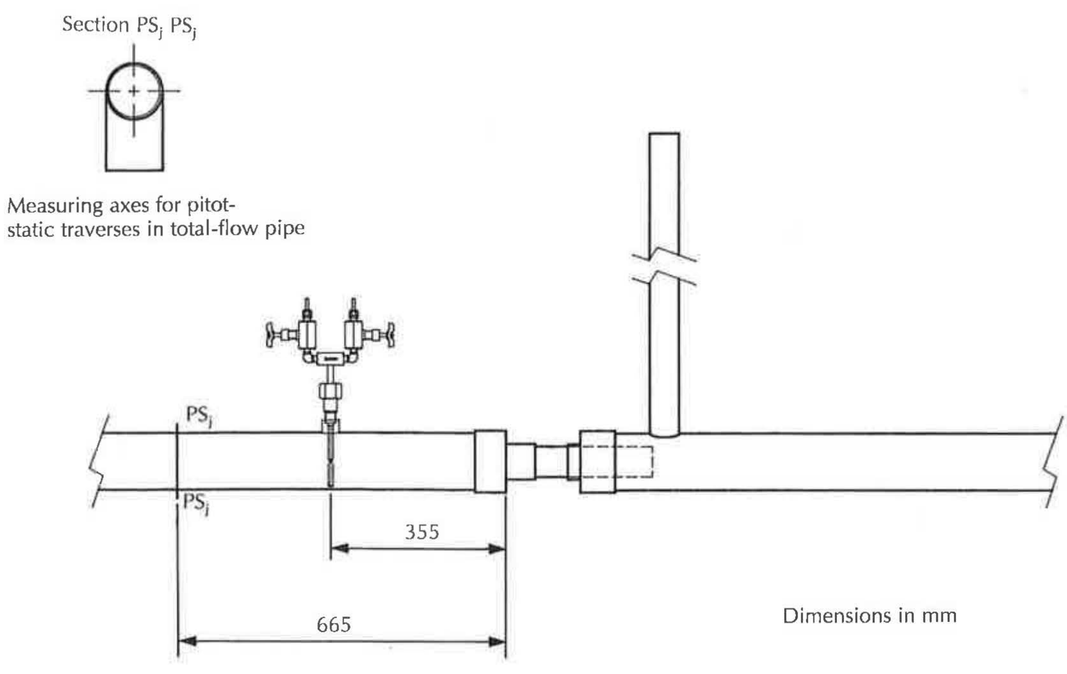

Figure 10 Installation of the Annubar in the jet-supply pipe

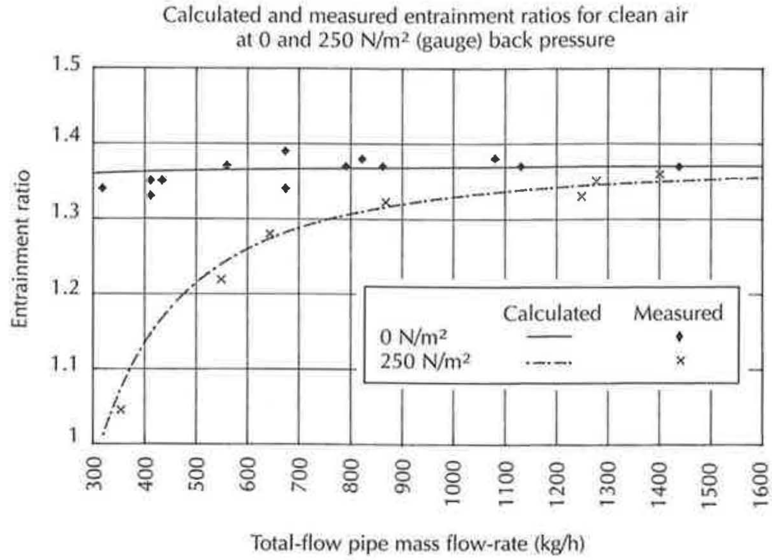

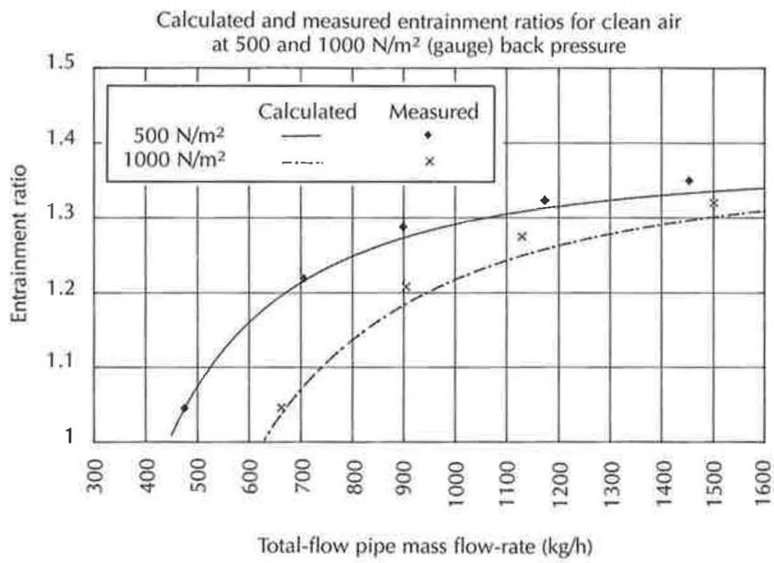

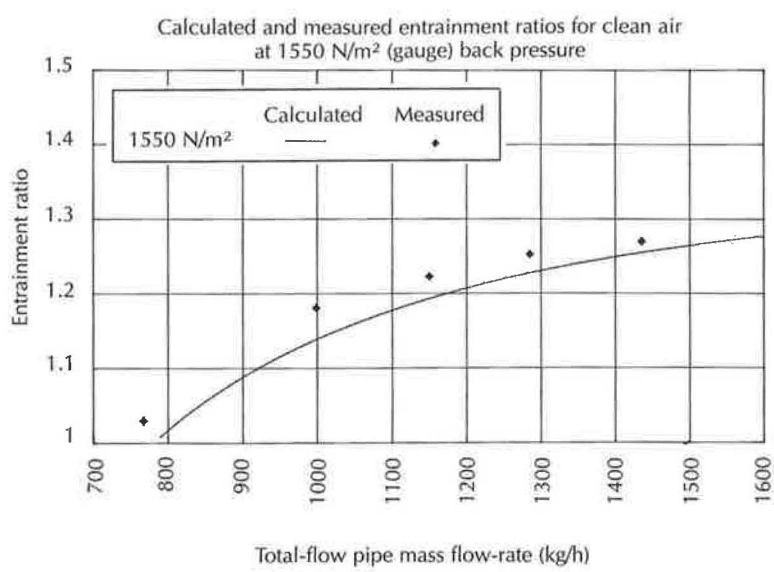

Figure 11 Calculated and measured entrainment ratios for clean air at different back pressures

Table 1 Injector entrainment ratios for clean air

Number	Total mass flow-rate (kg/h)	Entrainment ratio Measured	Calculated	% difference*	Absolute % difference
Back pressure (gauge) 0 N/m²					
1	318	1.34	1.360	1.471	1.471
2	263	1.37	1.359	−0.809	0.809
3	411	1.33	1.363	2.421	2.421
4	411	1.35	1.363	0.954	0.954
5	433	1.35	1.363	0.954	0.954
6	559	1.37	1.365	−0.366	0.366
7	674	1.34	1.367	1.975	1.975
8	674	1.39	1.367	−1.683	1.683
9	791	1.37	1.367	−0.219	0.219
10	822	1.38	1.368	−0.877	0.877
11	862	1.37	1.368	−0.146	0.146
12	1080	1.38	1.369	−0.804	0.804
13	1131	1.37	1.369	−0.073	0.073
14	1247	1.37	1.370	0.000	0.000
15	1438	1.37	1.370	0.000	0.000
Average error = 0.2%					
Absolute average error = 0.8%					
Back pressure (gauge) 250 N/m²					
1	354	1.05	1.074	2.235	2.235
2	549	1.22	1.240	1.613	1.613
3	644	1.28	1.274	−0.471	0.471
4	868	1.32	1.316	−0.304	0.304
5	1249	1.33	1.345	1.115	1.115
6	1277	1.35	1.346	−0.297	0.297
7	1401	1.36	1.350	−0.741	0.741
Average error = 0.4%					
Absolute average error = 1.0%					
Back pressure (gauge) 500 N/m²					
1	475	1.05	1.048	−0.191	0.191
2	706	1.22	1.207	−1.077	1.077
3	899	1.29	1.270	−1.575	1.575
4	1173	1.32	1.312	−0.610	0.610
5	1453	1.35	1.333	−1.275	1.275
Average error = 0.9%					
Absolute average error = 0.9%					
Back pressure (gauge) 1000 N/m²					
1	663	1.05	1.034	−1.547	1.547
2	905	1.21	1.180	−2.542	2.542
3	1130	1.28	1.246	−2.729	2.729
4	1501	1.32	1.298	−1.695	1.695
Average error = −2.1%					
Absolute average error = 2.1%					
Back pressure (gauge) 1550 N/m²					
1	767	1.03	0.985	−4.569	4.569
2	999	1.18	1.138	−3.691	3.691
3	1150	1.22	1.193	−2.263	2.263
4	1285	1.25	1.226	−1.958	1.958
5	1436	1.27	1.255	−1.195	1.195
Average error = −2.7%					
Absolute average error = 2.7%					
Average error for all readings = −1.036%					
Absolute average error for all readings = 1.528%					

*Calculated from Equation 24 (page 12).

MEASUREMENTS WITH SAWDUST

For tests conducted with sawdust entrainment, the air-flow measurements were made with the Annubar and carbon monoxide injection into the jet-supply pipe. Carbon monoxide concentrations were measured in the jet-supply and total-flow pipes. Details of this measuring technique are given in Appendix 3.

The entrainment ratio, with sawdust, is defined as:

$$E = \frac{m_{t,air} + m_{solid}}{m_j} \tag{25}$$

For these tests, back pressure was not controlled and was allowed to find its natural value dependent upon the air flow-rate and the restriction imposed by the particulate filter bag. The measured entrainment ratios were compared against the calculated values. The percentage difference calculated in accordance with Equation 24 showed random variation and no systematic effect was detected. The absolute average difference between the calculated and the measured values was found to be 3.1%. The results of these measurements and the calculated values are given in Table 2.

From the foregoing, it can be concluded that the theoretical procedures described in Section 2 are valid for the design of air injectors with particulate entrainment, provided that the effective densities of the particulate-laden gases in the total-flow pipe and the injected-fluid pipe are taken into account.

Table 2 Comparison of calculated and measured results for the air injector system

Number	Total mass flow-rate (kg/h)	Sawdust mass flow-rate (kg/h)	Measured back pressure (N/m^2)	Entrainment ratio		% difference	Absolute % difference
				Measured	Calculated		
1	399	115	158	1.47	1.44	−1.80	1.80
2	471	72	210	1.36	1.34	−1.42	1.42
3	471	163	200	1.57	1.51	−4.32	4.32
4	488	46	180	1.37	1.32	−3.71	3.71
5	720	114	400	1.37	1.37	0.07	0.07
6	731	170	380	1.51	1.44	−5.01	5.01
7	734	70	425	1.30	1.32	1.52	1.52
8	742	44	387	1.31	1.31	−0.38	0.38
9	967	73	690	1.25	1.31	4.80	4.80
10	968	121	668	1.33	1.36	1.85	1.85
11	977	43	680	1.25	1.29	3.33	3.33
12	991	165	689	1.41	1.39	−1.51	1.51
13	1173	46	1040	1.19	1.28	7.25	7.25
14	1207	109	985	1.26	1.33	5.55	5.55
15	1260	80	985	1.28	1.32	3.10	3.10
16	1302	189	936	1.46	1.39	−4.73	4.73
17	1496	84	1460	1.27	1.31	3.20	3.20
18	1552	118	1285	1.38	1.34	−2.68	2.68
19	1556	45	1500	1.27	1.30	2.01	2.01
20	1564	178	1580	1.40	1.36	−3.17	3.17
21	1583	83	1780	1.24	1.30	4.69	4.69
22	1633	56	1785	1.26	1.29	2.55	2.55
23	1703	183	1655	1.41	1.36	−3.45	3.45
24	1711	119	1665	1.37	1.34	−2.62	2.62

Average error = 0.2%
Absolute average error = 3.1%

Section 4

Application to the design of an air injector

Application of Equation 1 to the design of an air injector requires the following information:

1 Back pressure at the exit of the injector. The back pressure can be calculated from knowledge of the combustion chamber geometry, temperatures and flow-rates. The methods used for calculations of the various pressure losses are similar to those used in other fluid mechanics situations except that combustion chambers involve large temperature and density changes; proper recognition should be given to these. A detailed description of this subject is outside the scope of this publication and the reader is referred to standard texts on the topic (Thring, 1962; Trinks and Mawhiney, 1961; Etherington and Etherington, 1961). For this illustrative example, a back pressure of 1000 N/m^2 has been assumed.

2 Total air flow-rate ($m_{t,air}$) for this example has been assumed to be 1200 kg/h.

3 Particulate solids flow-rate (m_{solid}) has been assumed to be 120 kg/h.

4 Injected air flow-rate requirements can be obtained from consideration of the minimum air velocity required for dilute-phase transport of the particulates (solids-to-air mass ratios of less than 10:1). The minimum carrying velocity (V_{ch}) is given by Perry and Green (1984):

$$V_{ch} = 132.4\left(\frac{\rho_{solid}}{\rho_{solid} + C_2}\right)D_{solid}^{0.4} \qquad (26)$$

where ρ_{solid} is the density of the solid particle

D_{solid} is the maximum diameter of the particles to be transported. Both of these quantities are in SI units

C_2 is a constant and has a value of 998.

For sawdust particles of 440 kg/m^3 density and of 0.003 m diameter, the minimum carrying velocity is calculated to be 4 m/s. Rice husks, due to their shape and density, will be easier to transport than sawdust and the injector modelled on sawdust will operate satisfactorily with rice husks. For assured trouble-free operation with a short (0.5 m or less) vertical injected-fluid pipe with the solids being transported by gravity, an air velocity twice that of the minimum calculated should be used, i.e. the air velocity in the injected-fluid pipe should be 8 m/s. During this investigation, a 50 mm internal diameter pipe was used for the injected fluid. Air velocities as low as 6 m/s with solids flow-rates of up to 190 kg/h were tested with no operational difficulties. It is anticipated that difficulties are not likely to be encountered in 50 mm short vertical pipes with an air velocity of 8 m/s and solids flow-rates of up to around 300 kg/h. With this pipe size and air velocity, the injected air mass flow-rate ($m_{i,air}$) is calculated as 68 kg/h. This value should give an adequate design margin without imposing excessive entrainment requirements on the injector for applications in small-scale to medium-scale combustion systems for particulate biomass materials. For higher solids flow-rates, a larger pipe with air velocities of 10-12 m/s may prove to be more suitable.

5 The jet air mass flow-rate (m_j) is then given by the difference of $m_{t,air}$ and $m_{i,air}$. For this example, m_j is equal to 1132 (1200 – 68) kg/h.

6 The exit diameter of the injector is determined from considerations of the flame flash-back. Tests conducted at NRI indicate that, in order to prevent flame propagation into the air-solids conveyance pipe, minimum air velocities of the order of 12 m/s are required. However, for added safety margin, actual air velocities should be maintained above this value. Air velocities of 16–18 m/s have been found to be sufficient to prevent flash-back without incurring the penalties of excessively high velocities at the exit of the pipe. Therefore, for a given total air flow-rate, a maximum injector outlet pipe diameter can be determined. For this example, the exit diameter of the injector is found to be 149 mm for an air velocity of 16 m/s and a total air flow-rate of 1200 kg/h.

With the specific requirements outlined above for the injector and the information derived from these, Equation 1 can be solved to give the size of jet required. By substituting for $Q = m/\rho$ and rearranging, Equation 1 is written as:

$$A_j = \frac{(m_j^2/\rho_j C_j)}{\left[(P_t - P_i) + S_{12}\frac{m_t^2}{2\rho_t A_t^2}\right]A_t + \frac{m_t^2}{\rho_t A_t}} \qquad (27)$$

and

$$D_j = \sqrt{\frac{4A_j}{\pi}} = 1.128\sqrt{A_j} \qquad (28)$$

S_{12}, P_i and ρ_t have been defined previously in Equations 2, 3 and 11 respectively.

A BASIC computer program to calculate the jet diameter as a function of the injector outlet diameter (maximum outlet diameter being consistent with the 16 m/s air velocity requirement at the exit) is given in Appendix 5. In most cases an optimum combination of total-flow pipe diameter and jet diameter will exist. For the optimized design, the jet diameter will be a maximum and both the jet air power and the jet total pressure (sum of the static and dynamic pressures) at the jet exit will be at a minimum. The air power at the jet exit is calculated from the consideration that the jet air needs to be raised from ambient pressure to the jet total pressure and is given by:

$$W_j = Q_j\, P_j \qquad (29)$$

where W_j is the air power at the jet exit, in watts

Q_j is the volumetric flow-rate, in m^3/s

P_j is the total pressure, in N/m^2

Although air power at the jet exit is related to the fan-power requirements, pressure losses upstream of the jet exit must also be taken into account. Denoting these pressure losses as $P_{j,loss}$ and taking a typical centrifugal fan efficiency of 60%, the fan-power requirements are given by:

$$\text{Fan power} = \frac{1}{0.6}\, Q_j\, (P_j + P_{j,loss}) \qquad (30)$$

Care should be taken in the design of the pipe work upstream of the injector jet to the fan outlet. The best design will be a single-step shallow-angle (less than 30°) reducer from the fan outlet to the jet and a short connecting pipe from the reducer to the injector jet.

Performance of the injector can be improved further if a diffuser is incorporated at the end of the total-flow pipe. Such an arrangement is shown in Figure 12 with the data applicable to the present example. The results obtained from the program given in Appendix 5 are plotted in Figure 13 for a parallel injector (without a diffuser) and for injectors with diffusers of 14°, 30° and 45° included

Diffuser pressure coefficient = $S_d = \xi\,(1 - A_t/A_f)^2$
Diffuser pressure loss based on upstream velocity

ω	3°	5-8°	10°	14°	20°	30°	45°	60°	90°
ξ	0.18	0.14	0.16	0.25	0.45	0.7	0.95	1.1	1.0

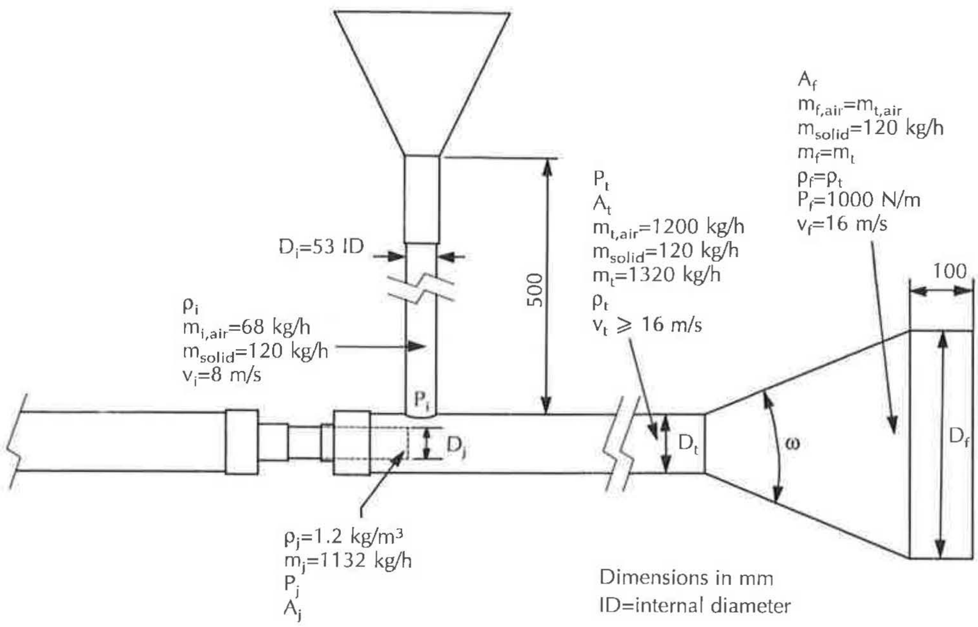

Figure 12 Injector used for present example

angle. These results show that the power and pressure requirements for the fan are significantly reduced for injectors with a diffuser compared to those for the parallel injector. Parallel-injector design optimized for the fan pressure and fan power will result in much higher exit velocities and consequently a delayed flame ignition zone. Inclusion of a diffuser in the injector provides the means for controlling injector exit velocities to 16 m/s. For injectors with a diffuser, the total-flow pipe back pressure term (P_t) in Equation 27, should be substituted by the following to take into account the diffuser pressure losses:

$$P_t = P_f + \frac{m_t^2}{2\rho_t A_t^2}\left[\xi\left(1 - \frac{A_t}{A_f}\right)^2 + \left(\frac{A_t}{A_f}\right)^2 - 1\right] \qquad (31)$$

where P_f is the back pressure at the exit of the injector

$A_t = A_f$ for a parallel injector and consequently

$P_t = P_f$

ξ is the coefficient for the diffuser pressure-loss term. This was obtained from literature (Rose and Cooper, 1977).

During the test work, the conical funnel shown in Figure 14 was used to collect the solids flow from the vibratory hopper. This design was found to operate without blockages, and a similar arrangement is therefore recommended for other applications.

Finally, the design chosen for the injector should be checked for the jet-impingement point in relation to the injected-fluid pipe. It is felt that a clearance greater than 0.5 jet diameters will be adequate. The clearance distance can be checked from the following:

$$L - D_i \geq \frac{1}{2}D_j \qquad (32)$$

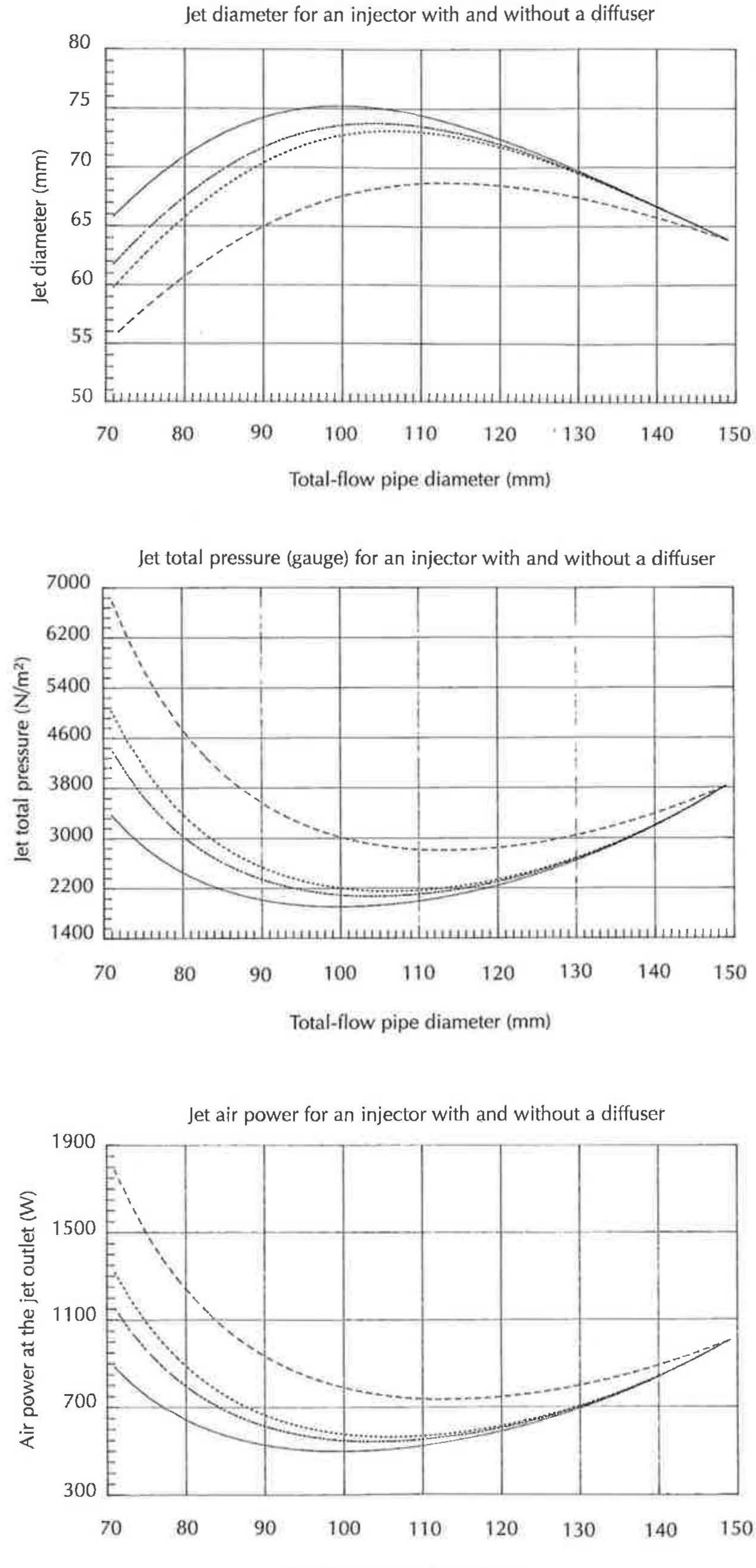

Key
14° diffuser ——— 45° diffuser ·······
30° diffuser -·-·-·- without diffuser - - - -

Air flow-rate 1200 kg/h. Solids flow-rate 120 kg/h.
Back pressure 1000 N/m^2. Diffuser diameter 150 mm.

Figure 13 Injector performance with diffusers of 14°, 30° and 45° included angle and without a diffuser

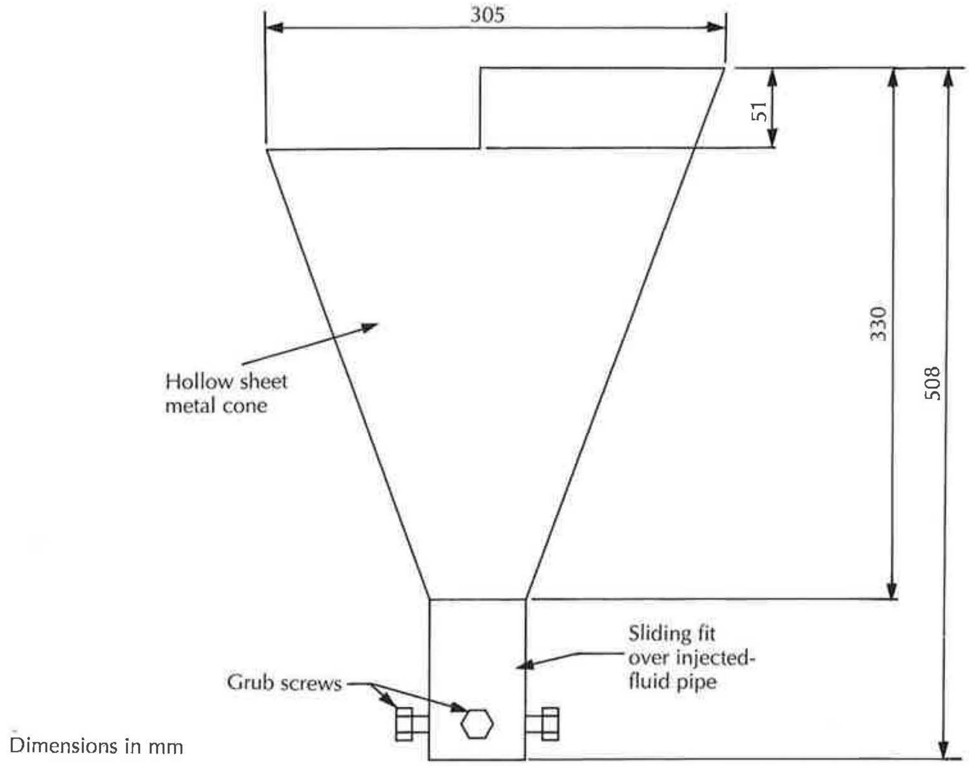

Figure 14 Conical funnel for the solids flow from vibratory table feeder

where L is given by:

$$L = \frac{(D_t - D_j)}{2 \text{ Tan } 10°} = 2.84\ (D_t - D_j) \tag{33}$$

The above equation is defined from the jet angle of 20° given in Section 2; L is the axial distance from the jet exit to the point of jet impingement on the total-flow pipe. If the above criterion is not fulfilled by the optimized design obtained from the program in Appendix 5, then the jet diameter should be reduced.

The program given in Appendix 4 can be used to evaluate the performance of the injectors with changed values of pipe sizes, flow-rates and back pressures.

Section 5

Conclusions

This work has extended applications of the well-established theory developed for clean gases to the entrainment of particulate solids.

A simplified mathematical model of injectors for entrainment of particulate-laden gases, with low solids-to-air ratios, has been developed and experimentally verified.

Procedures optimized for minimum fan power and fan pressure have been developed for the design of injectors for particulate biomass combustion systems.

Based on this work, a suitable low-pressure air injector for particulate conveyance was developed for use with a rice-husk fuelled suspension burner and was subsequently operated successfully at a commercial rice mill in Sri Lanka.

This work has augmented NRI's first-hand experience in the handling of abrasive biomass material and has provided data to assist in the design, development and application of new and improved suspension burners for particulate biomass in agricultural and forestry industries. It forms part of a wider programme of work to enable developing countries to derive greater benefit from their resources through the use of sustainable and more environmentally harmonious technologies.

References

BEAGLE, E. C. (1978) Rice husk conversion to energy. *FAO Agricultural Services Bulletin* No. 31. Rome: Food and Agricultural Organization of the United Nations.

BEER, J. M. and CHIGIER, N. A. (1972) *Combustion Aerodynamics.* London: Applied Science Publishers.

COKER, K. (1991) Sizing process piping for single-phase fluids. *The Chemical Engineer,* 10 Oct 1991: 19-25.

COLEBROOK, C. F. (1939) Turbulent flow in pipes, with particular reference to the transition region between smooth and rough pipe laws. *Journal of the Institute of Civil Engineers,* **11**: 133-156.

ETHERINGTON, H. and ETHERINGTON, G. (1961) *Modern Furnace Technology.* London: Charles Griffin.

FAO (1989) FAO Year Book, Forest Products, *FAO Forestry Series* No. 24, *FAO Statistics Series* No. 97. Rome: Food and Agricultural Organization of the United Nations.

FAO (1990) FAO Production Year Book, Vol. 44, *FAO Statistics Series* No. 99. Rome: Food and Agricultural Organization of the United Nations.

FRANCIS, W. E. (1956) Forced recirculation in industrial gas appliances, Gas Council Research Communication GC 34. *Transactions of the Institute Gas Engineers,* **106**: 483-529

FRANCIS, W. E. (1964) A generalized procedure for optimum design of injectors, ejectors and jet pumps. Gas Council Research Communication GC 101. *Journal of the Institute Gas Engineers,* **4**: 399-414.

GELDART, D. (1986) *Gas Fluidization Technology.* Chichester: John Wiley.

KROLL, A. E. (1947) The design of jet pumps. *Journal of Chemical Engineering Progress,* February: 21-24.

PERRY, R. H. and GREEN, D. (1984) *Perry's Chemical Engineer's Handbook.* New York: McGraw Hill.

PRITCHARD, R., GUY, J. J. and CONNOR, N. E. (1977) *Industrial Gas Utilization.* Epping: Bowker.

ROBINSON, A. P. (1991) The design and development of a suspension burner system for particulate forestry and agricultural residues. *Natural Resources Institute Bulletin,* **41**, Chatham, UK: Natural Resources Institute.

ROBINSON, A. P. and BREAG, G. R. (1992) The construction and operation of a suspension system using particulate wood waste as a fuel. *Natural Resources Institute Rural Technology Guide,* **17**: Chatham, UK: Natural Resources Institute.

ROBINSON, A. P., HOLLINGDALE, A. C. and REUPKE, P. (1992) The construction and operation of a rice husk burner. *Natural Resources Institute Rural Technology Guide,* **18**. Chatham, UK: Natural Resources Institute.

ROSE, J. W. and COOPER, J. R. (1977) *Technical Data on Fuels.* London: The British National Committee, World Energy Conference.

THRING, M. W. (1962) *Science of Flames and Furnaces*. London: Chapman and Hall.

TRINKS, W. and MAWHINEY, M. H. (1961) *Industrial Furnaces* Vol. 1 and Vol. 2. New York and London: John Wiley.

Appendices

APPENDIX 1 PRESSURE DROPS FOR DILUTE-PHASE PNEUMATIC TRANSPORT OF SOLIDS

For dilute-phase particle-laden air of solids-to-gas ratios encountered during this work, it was assumed that the pressure drops for the injected-fluid pipe and total-flow pipe could be calculated from the properties of clean air, Fanning friction factors and the effective densities of the particle-laden air. This assumption was tested against a more detailed analysis (Perry and Green, 1984; Geldart, 1986). The total pressure drop in the vertical injected-fluid pipe can be calculated as a sum of the following individual pressure terms:

1 For acceleration of the gas to the carrying velocity:

$$\Delta P_1 = \frac{1}{2}\rho_{d,air}\, v_{air}^2 \tag{1.1}$$

where $\rho_{d,air}$ is the dispersed gas density and is the mass of the gas per unit volume of the solids-gas mixture and can be calculated from:

$$\rho_{d,air} = m_{air} / (m_{solid}/\rho_{solid} + m_{air}/\rho_{air}) \tag{1.2}$$

v_{air} is the air velocity in the pipe and is given by the volume flow-rate of the air divided by the cross-sectional area of the pipe

ρ_{solid} is the density of the solid particles.

2 For acceleration of the solid particles:

$$\Delta P_2 = \rho_{d,solid}\, v_{solid}^2 \tag{1.3}$$

where $\rho_{d,solid}$ is the dispersed density of solids and is the mass of the solids per unit volume of the solids-gas mixture, and can be calculated from:

$$\rho_{d,solid} = m_{solid} / (m_{solid}/\rho_{solid} + m_{air}/\rho_{air}) \tag{1.4}$$

The actual velocity of the solids (v_{solid}) for solids-to-air mass ratios less than 5, is given by:

$$v_{solid} = v'_{air}\,(1 - C_i\, D_{solid}^{0.3}\, \rho_{solid}^{0.5}) \tag{1.5}$$

where C_i is a constant = 0.0639

D_{solid} is the diameter of the solid particles and was taken to be .003 m for sawdust

ρ_{solid} is the density of the solid particles and was taken as 440 kg/m^3

v'_{air} is the superficial air velocity and is given by:

$$v'_{air} = \frac{\rho_{d,air}}{\rho_{air}}\, v_{air} \tag{1.6}$$

3 For friction between gas and pipe wall:

$$\Delta P_3 = \frac{4\, f_{air}\, L\, \rho_{d,solid}\, v_{air}^2}{2D} \tag{1.7}$$

where f_{air} is the Fanning friction factor described in Section 2

L and D are the pipe length and diameter respectively and are in metres.

4 For combined friction between particles and the pipe wall, between gas and the particles and between particles, the pressure term is given by:

$$\Delta P_4 = \frac{4\, f_{solid}\, L\, \rho_{d,solid}\, v^2_{solid}}{2D} \quad (1.8)$$

where f_{solid} is given by:

$$4f_{solid} = \frac{3\, \rho_{air}\, D\, C}{2\, \rho_{solid}\, D_{solid}} \left(\frac{v_{air} - v_{solid}}{v_{solid}}\right)^2 \quad (1.9)$$

C is the drag coefficient and can be calculated from the correlations or read from graphs (Perry and Green, 1984), as a function of the particle Reynolds number Re_{solid}:

$$Re_{solid} = \frac{D_{solid}\,(v_{air} - v_{solid})\,\rho_{air}}{\mu_{air}} \quad (1.10)$$

Correlations used to calculate the particle drag coefficient are as follows:

$$C = \frac{24}{Re_{solid}} \qquad \text{for } Re_{solid} < 0.1$$

$$= \left(\frac{24}{Re_{solid}}\right)(1 + 0.14Re^{0.7}_{solid}) \qquad \text{for } 0.1 < Re_{solid} < 1000$$

$$= 0.445 \qquad \text{for } 1000 < Re_{solid} < 350{,}000$$

5 For support of a column of gas in a vertical pipe:

$$\Delta P_5 = \rho_{d,air}\, L\, g \quad (1.11)$$

where g is the acceleration due to gravity and is equal to 9.8 m/s^2.

6 For support of the solids in a vertical pipe:

$$\Delta P_6 = \rho_{d,solid}\, L\, g \quad (1.12)$$

7 Pressure loss for entrance of the fluid from a large reservoir to a square-edged pipe, taking a pressure-loss coefficient (Rose and Cooper, 1977) of 0.5, is given by:

$$\Delta P_7 = \frac{1}{4}\, \rho_{air}\, v^2_{air} \quad (1.13)$$

For the injected-fluid pipe, the total pressure drop ΔP_8 is given by the sum of ΔP_1 to ΔP_7 above:

$$\Delta P_8 = \Delta P_1 + \ldots. + \Delta P_7 \quad (1.14)$$

ΔP_8 was calculated for a unit length of pipe and was compared against the pressure drop (ΔP_i) calculated from the simplified assumption made in Section 2 that ΔP_i is given by:

$$\Delta P_i = \left(0.5 + \frac{4fL}{D} + 1\right) \frac{1}{2}\, \rho_i\, v^2_{air} \quad (1.15)$$

The calculations were made for a solids flow-rate of 200 kg/h and a range of air flow-rates. These flow-rates encompass situations likely to be encountered in application of the injectors to small-scale to medium-scale particulate biomass combustion systems. The results are given in Figure 1.1. These results show that, for low solids-to-air ratios, the assumptions made in Section 2 are valid for the design of injectors for small-scale to medium-scale combustion systems.

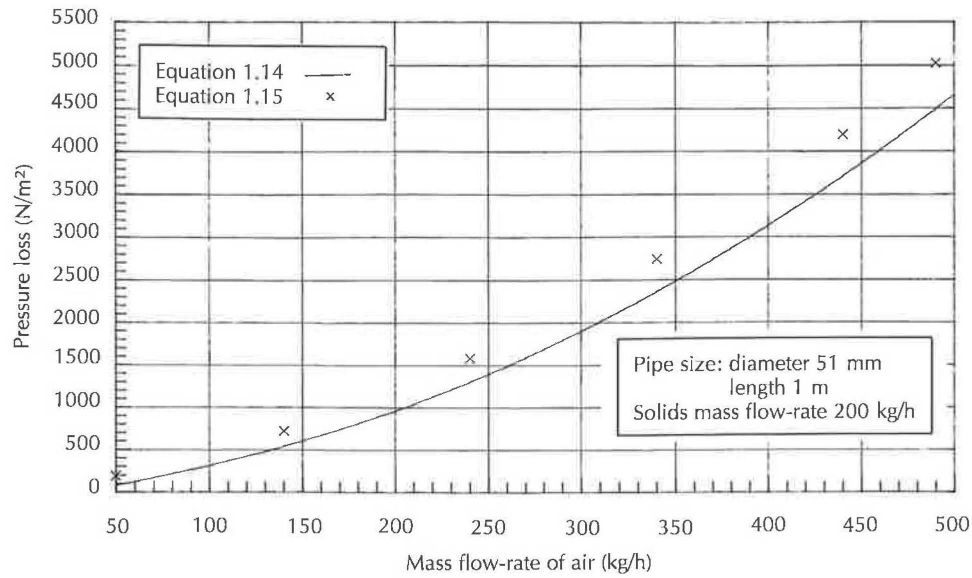

Figure 1.1 Comparison of the pressure drop for the injected-fluid pipe (calculated from Equations 1.14 and 1.15)

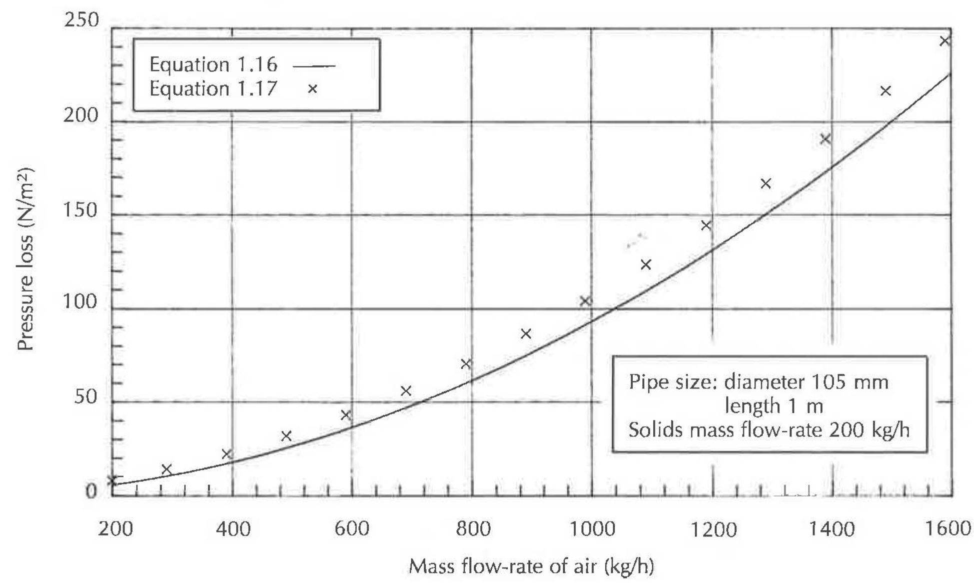

Figure 1.2 Comparison of the friction pressure loss in the total-flow pipe (calculated from equations 1.16 and 1.17)

In Section 2, the assumption was made that the frictional pressure loss in the total-flow pipe can be approximated by:

$$\Delta P = \frac{4fL}{D}\left(\frac{1}{2}\rho_t v_t^2\right) \tag{1.16}$$

A more rigorous value for this pressure loss, ΔP_9, would be obtained by a sum of ΔP_3 and ΔP_4 above, i.e.:

$$\Delta P_9 = \Delta P_3 + \Delta P_4 \tag{1.17}$$

The pressure losses calculated using Equations 1.16 and 1.17 are compared in Figure 1.2. For practical purposes, the two values are close and the assumption made in Section 2 can be used for design purposes.

APPENDIX 2 AIR-FLOW MEASUREMENTS WITH AN 'ANNUBAR'

An 'Annubar' is a differential pressure flow metering instrument and relies on the fact that when an obstruction is placed in the fluid flow path then a difference exists between the leading stagnation point pressure and trailing stagnation point pressure. The differential pressure generated is proportional to the square of the flow-rate in accordance with Bernoulli's theorem. The pressure at the trailing stagnation point also depends on the flow separation point on the obstruction. The shape of the Annubar causes the flow to separate at a fixed point on the Annubar and this ensures predictable results within the instrument's operating range. The pressure tappings in the instrument are designed to give an averaged value over the pipe diameter. The following equation is given by the instrument manufacturers for the relationship between differential pressure indicated by the instrument and the fluid mass flow-rate:

$$\Delta P = C_f \, 6.2652 \times 10^{-8} \frac{1}{\rho} \left(\frac{m}{KD^2} \right)^2 \qquad (2.1)$$

where ρ is the density of the fluid at the point of flow-measurement and is in kg/m^3

m is the mass flow-rate in kg/h

D is the pipe diameter in m

ΔP is the differential-pressure in N/m^2

K is the instrument constant with a value of 0.6242 for the particular model used here

C_f represents a combination of minor corrections required for the Reynolds number dependence, gas expansion, thermal expansion and the gauge location.

For the present study C_f was evaluated by calibrating the Annubar *in situ* with pitot-static measurements. The pitot-static measurements were made at the injector exit and during these measurements the injected-fluid pipe was blanked. The mass flow-rates calculated from Equation 2.1 are plotted against the differential pressure in Figure 2.1 and are compared with the pitot-static measurements in Figure 2.2.

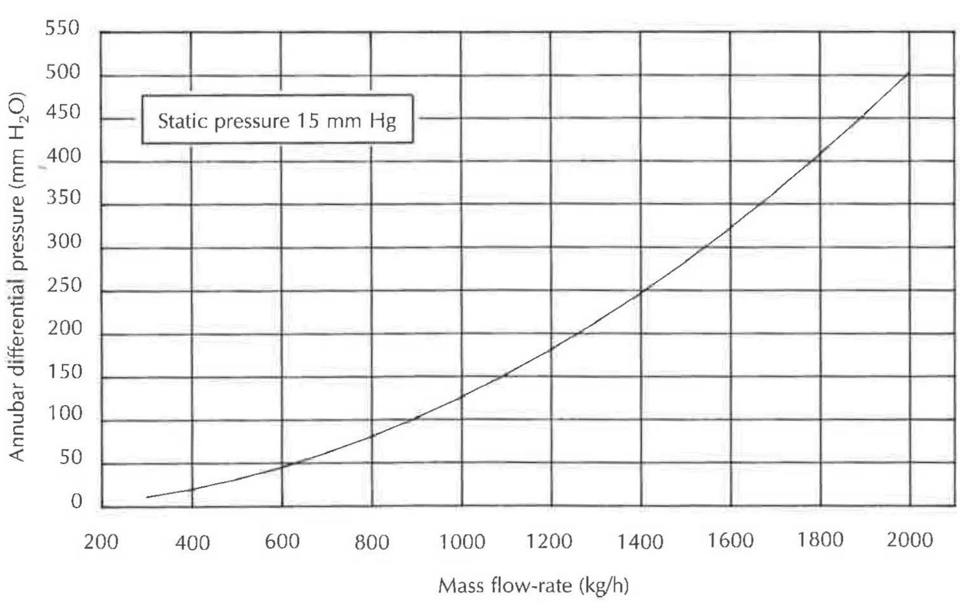

Figure 2.1 Flow-rate and differential pressure characteristics for the Annubar

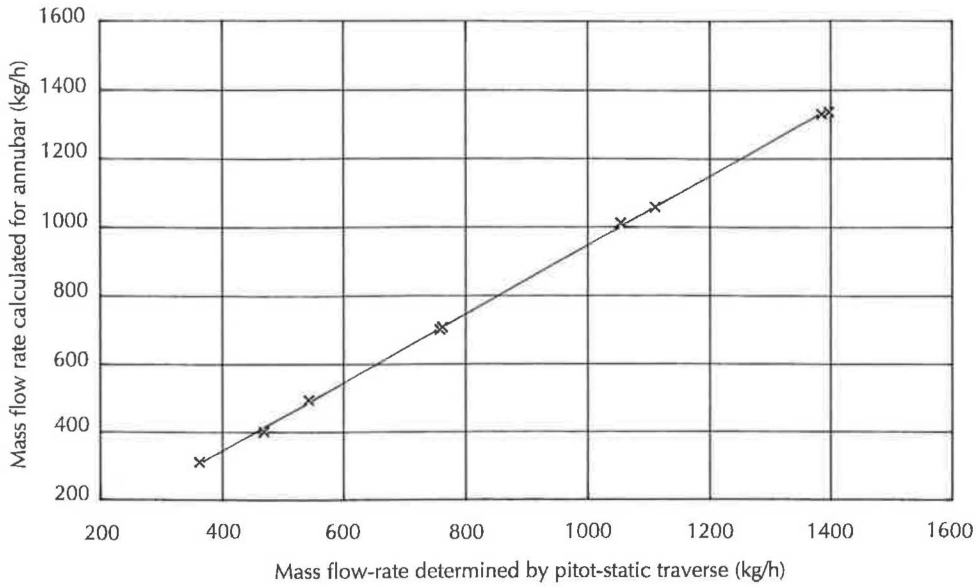

Figure 2.2 Comparison of actual flow-rate determined by pitot-static traverse with that calculated for the Annubar

APPENDIX 3 AIR-FLOW MEASUREMENTS WITH CARBON MONOXIDE INJECTION TECHNIQUE

The measurement of air flows in dust-laden gases is difficult with conventional techniques and prone to errors. Due to this difficulty the air flow in the total-flow pipe was measured with a carbon monoxide (CO) injection technique. Carbon monoxide was injected into the jet fluid and its concentration measured sufficiently far downstream from the CO injection point to allow total mixing. The jet air flow-rate was measured with the Annubar. From the above two measurements and measurement of the CO concentration in the total-flow pipe, the air flow-rate in the total-flow pipe can be calculated. The concentrations of CO in the jet pipe and total-flow pipe are related to the volume flow-rates of CO and air by the following:

$$c_{j,co} = \frac{Q_{co}}{Q_{j,air}} \quad (3.1) \text{ and } \quad c_{t,co} = \frac{Q_{co}}{Q_{t,air}} \quad (3.2)$$

Since the volume flow-rate of CO, Q_{co} remains constant through the injector system, the ratio of the jet-fluid and the total-fluid volume flow-rates is given by the ratio of the CO concentrations in the two pipes, i.e.:

$$\frac{Q_{t,air}}{Q_{j,air}} = \frac{c_{j,co}}{c_{t,co}} \quad (3.3)$$

From knowledge of the static pressure and temperature of the two streams, the densities can be calculated and the mass flow-rates and the entrainment ratio can be derived as:

$$E = \frac{m_{t,air}}{m_j} = \frac{Q_{t,air}\,\rho_t}{Q_{j,air}\,\rho_j} = \frac{c_{j,co}}{c_{t,co}}\;\frac{\rho_t}{\rho_j} \quad (3.4)$$

The radial concentration profiles taken for the CO in the two pipes showed uniform concentrations of CO across the diameters of the two pipes indicating perfect mixing and, therefore, a single sampling point was used in all of these measurements. The arrangement used for measurements with CO injection is shown in Figure 3.1.

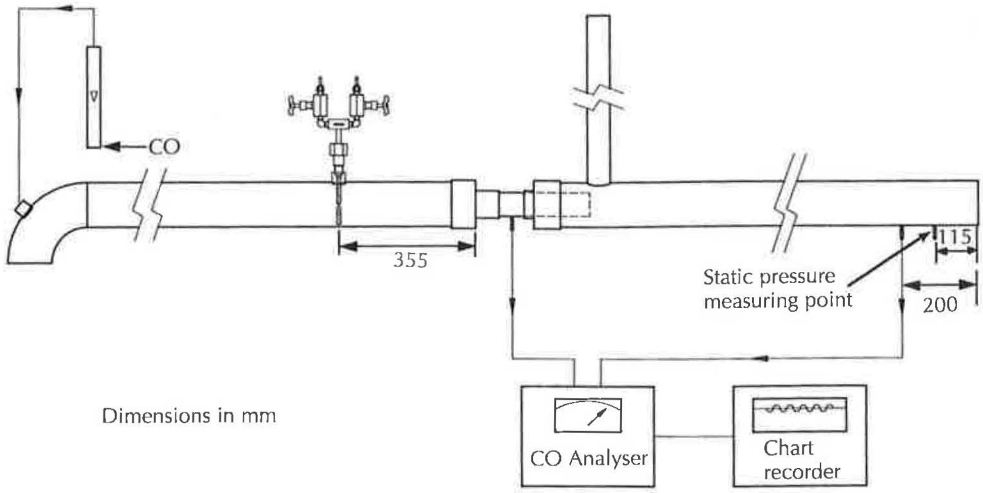

Figure 3.1 Arrangements for measurements of air flow-rates with carbon monoxide injection technique

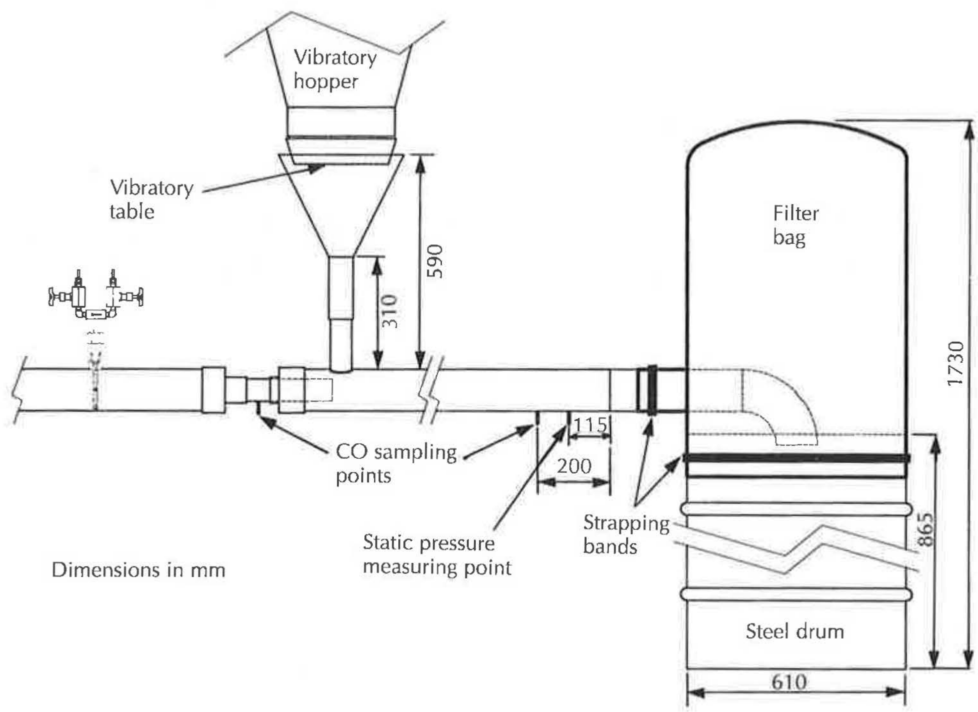

Figure 3.2 Arrangement for flow measurements with sawdust entrainment

For the tests conducted with sawdust, measurements were made in a similar manner and the arrangement used for sawdust collection is shown in Figure 3.2. Entrainment ratios were calculated from the jet mass flow-rate measured with the Annubar, and the CO concentration ratio was used to calculate the mass flow-rate of the air in the total-flow pipe. The sawdust flow-rate was determined from the quantity of sawdust collected in the filter bag during the tests. The entrainment ratio for the injector, including the sawdust, is then defined as:

$$E = \frac{m_{t,air} + m_{solid}}{m_j} \tag{3.5}$$

The CO concentrations were measured with an infrared CO analyser linked to a chart recorder. The stated accuracy of the CO analyser was better than 1% full-scale deflection. With a full-scale deflection of 1000 ppm, an accuracy of at least

±10 ppm can be expected for the CO concentration measurements. The infrared analyser was calibrated with a certified test gas of 435 ppm CO concentration. The concentration of CO within the jet fluid was maintained at approximately 450 ppm and this led to CO concentrations of the order of 350 ppm or greater in the total-flow pipe. This gives an accuracy better than ±2.8% for all CO concentration measurements. The Annubar accuracy stated by the manufacturers is ±1%. Therefore error for flow-measurement with the CO injection technique is not likely to exceed ±6.6%. For this work the Annubar was calibrated *in situ* and the infrared analyser was calibrated with a certified calibrant gas of CO concentration close to that measured in the two pipes, therefore an accuracy much better than ±6.6% can be expected for the actual flow measurements.

APPENDIX 4 PROGRAM FOR INJECTOR PERFORMANCE

```
10 CLS
20 REM CALCULATIONS WITH DIFFUSER
30 REM INPUT BASIC INJECTOR GEOMETRY
40 PRINT "PLEASE ENTER BASIC INJECTOR GEOMETRY"
50 INPUT "ENTER LENGTH OF TOTAL FLOW TUBE (m) ", LT
60 INPUT "ENTER LENGTH OF INJECTED FLUID TUBE (m) ", LI
70 PRINT
80 INPUT "ENTER DIAMETER OF TOTAL FLOW TUBE (mm) ", DT
90 INPUT "ENTER DIAMETER OF INJECTED FLUID TUBE (mm) ", DI
100 INPUT "ENTER DIAMETER OF JET FLUID TUBE (mm) ", DJ
110 PRINT
120 INPUT "DOES INJECTOR HAVE A DIFFUSER (Y/N) ", Q1$
130 IF Q1$ = "Y" THEN GOTO 150
140 IF Q1$ = "y" THEN GOTO 150 ELSE GOTO 160
150 GOSUB 1900
160 CONTROL = 0
170 DF = DT
180 PRINT
190 INPUT "ENTER TOTAL AIR FLOW (kg/h) ", MTAIRH
200 INPUT "ENTER SOLIDS FLOW RATE (kg/h) ", SOLIDH
210 PRINT
220 INPUT "ENTER STATIC BACK PRESSURE AT INJECTOR OUTLET (N/m^2) ";
PF
230 REM ------------------------------------
240 REM BASIC DATA MINIPULATION
250 DTA = DT / 1000
260 DIA = DI / 1000
270 DJA = DJ / 1000
280 DFA = DF / 1000
290 PI = 3.1415927#
300 AT = PI * (DTA / 2) ^ 2
310 AI = PI * (DIA / 2) ^ 2
320 AJ = PI * (DJA / 2) ^ 2
330 AF = PI * (DFA / 2) ^ 2
340 MTAIR = MTAIRH / 3600
350 SOLID = SOLIDH / 3600
360 REM
370 REM PIPE ROUGHNESS FACTORS
380 ROUGHT = .0457 / DT
390 ROUGHI = .0457 / DI
400 REM
410 REM FLUID DENSITY kg/m ^ 3
420 RHOJ = 1.2
430 RHOT = RHOJ * (1 + SOLID / MTAIR)
```

```
440 REM LOSS COEFFICIENTS FOR INJECTED PIPE
450 ECOEFF = .5
460 HLCOEFF = 1
470 WLCOEFF = .35
480 CJ = .95
490 REM FLUID VISCOSITY IN Ns/m^2
500 VISCO = 1.8455E-05
510 REM  - - - - - - - - - - - - - - - - - - - - - - - - - - - -
520 TEMP1 = (AT / AF)
530 TEMP2 = (MTAIR + SOLID) ^ 2 / (2 * RHOT * AT ^ 2)
540 TEMP3 = (AT / AF) ^ 2
550 TEMP4 = ZETA * (TEMP1 – 1) ^ 2
560 PT = PF + CONTROL * TEMP2 * (TEMP4 + TEMP3 – 1)
570 REM  - - - - - - - - - - - - - - - - - - - - - - - - - - - -
580 REM CALCULATE TOTAL FLOW PIPE VELOCITY
590 VT = (MTAIR + SOLID) / (RHOT * AT)
600 REM CALCULATE TOTAL FLOW TUBE REYNOLDS NUMBER
610 RET = RHOT * VT * DTA / VISCO
620 ROUGH = ROUGHT
630 RE = RET
640 GOSUB 1720
650 FT = FFF
660 S12 = 4 * FT * LT / DTA
670 BETA = (.5 * S12 + 1) / RHOT
680 GAMMA = 1 / (RHOJ * CJ) * (AT / AJ)
690 THETA = PT * AT ^ 2
700 TCOEFF = ECOEFF + HLCOEFF + WLCOEFF
710 MJ = 0
720 MSOLID = 0
730 CHK = 1
740 GOSUB 1570
750 IF CHK <= 0 THEN GOTO 1560
760 REM ******RETURN FROM SUB 2000*************
770 COUNT = 0
780 MI = MT – MJNEW
790 VI = MI / (RHOI * AI)
800 REI = RHOI * VI * DIA / VISCO
810 ROUGH = ROUGHI
820 RE = REI
830 GOSUB 1720
840 FI = FFF
850 WLCOEFF = 4 * FI * LI / DIA
860 TCOEFF = ECOEFF + HLCOEFF + WLCOEFF
870 MSOLID = SOLID
880 CHK = 1
890 MJ = MJNEW
900 COUNT = COUNT + 1
910 GOSUB 1570
920 IF CHK <= 0 THEN GOTO 1560
930 REM ******* RETURN FROM SUB 2000 *********
940 DELTA = ABS(MJNEW – MJ)
950 IF DELTA > .00001 THEN GOTO 780
960 MJH = MJNEW * 3600
970 MIH = MTAIRH + SOLIDH – MJH
980 MIAIRH = MIH – SOLIDH
990 ERATIO = (MTAIRH + SOLIDH) / MJH
1000 MI = MT – MJNEW
1010 VI = MI / (RHOI * AI)
1020 REI2 = RHOI * VI * DIA / VISCO
1030 PLOSSI = -TCOEFF * VI ^ 2 * RHOI / 2
1040 QJ = MJNEW / RHOJ : VJ = QJ / AJ
```

```
1050 PJ = PLOSSI + .5 * RHOJ * VJ ^ 2
1060 APOWER = QJ * PJ
1070 REM - - - - - - - - - - - - - - - - - - - - - - - - - - - - -
1080 LPRINT "BASIC INJECTOR GEOMETRY"
1090 LPRINT " - - - - - - - - - - - - - -"
1100 LPRINT "LENGTH OF TOTAL FLOW TUBE ="; LT; " m"
1110 LPRINT "LENGTH OF INJECTED FLUID TUBE ="; LI; " m"
1120 LPRINT
1130 LPRINT "DIAMETER OF THE TOTAL FLOW TUBE ="; DT; " mm"
1140 LPRINT "DIAMETER OF THE INJECTED FLUID TUBE ="; DI; " mm"
1150 LPRINT "DIAMETER OF THE JET FLUID TUBE ="; DJ; " mm"
1160 LPRINT "DIAMETER OF THE DIFFUSER EXIT ="; DF; " mm"
1170 LPRINT
1180 LPRINT "DIFFUSER ANGLE ="; ANG1; " DEGREES"
1190 LPRINT
1200 LPRINT "DETAILS OF TOTAL FLOW TUBE"
1210 LPRINT "  - - - - - - - - - - - - - - - -"
1220 LPRINT "TOTAL AIR FLOW RATE ="; MTAIRH; " kg/h"
1230 LPRINT "TOTAL FLOW PIPE REYNOLDS NUMBER ="; RET
1240 LPRINT "TOTAL FLOW PIPE FANNING FRICTION FACTOR ="; FT
1250 LPRINT
1260 LPRINT "DETAILS FOR THE INJECTED FLUID PIPE"
1270 LPRINT " - - - - - - - - - - - - - - - - - - - - - -"
1280 LPRINT "INJECTED AIR FLOW RATE ="; MIAIRH; "kg/h"
1290 LPRINT "TOTAL INJECTED FLOW RATE ="; MIH; " kg/h"
1300 LPRINT "INJECTED PIPE VELOCITY ="; VI; " m/s"
1310 LPRINT "INJECTED AIR FLOW RATE ="; MIAIRH; "kg/h"
1320 LPRINT "TOTAL INJECTED FLOW RATE ="; MIH; " kg/h"
1330 LPRINT "INJECTED PIPE PRESSURE ="; PLOSSI; " N/m^2"
1340 LPRINT "INJECTED PIPE REYNOLDS NUMBER ="; REI
1350 LPRINT "INJECTED PIPE FANNING FRICTION FACTOR ="; FI
1360 LPRINT
1370 LPRINT "DETAILS FOR THE JET FLUID TUBE"
1380 LPRINT "- - - - - - - - - - - - - - - - -"
1390 LPRINT "JET FLOW RATE ="; MJH; " kg/h"
1400 LPRINT "PRESSURE REQUIRED FOR JET FLOW ="; PJ; " N/m^2"
1410 LPRINT "AIR POWER FOR JET ="; APOWER; " W"
1420 LPRINT
1430 LPRINT "PARTICULATE SOLIDS DATA"
1440 LPRINT "- - - - - - - - - - - - - - -"
1450 LPRINT "SOLIDS FLOW RATE ="; SOLIDH; " kg/H"
1460 LPRINT
1470 LPRINT "MISCELLANEOUS DATA"
1480 LPRINT "- - - - - - - - - - - -"
1490 LPRINT "STAIC BACK PRESSURE AT THE INJECTOR OUTLET ="; PF; "
Pa"
1500 LPRINT "NUMBER OF ITERATIONS CONDUCTED IS "; COUNT
1510 LPRINT
1520 LPRINT
1530 LPRINT "ENTRAINMENT RATIO "; ERATIO
1540 LPRINT "  - - - - - - - - - - - - - - - -"
1550 LPRINT:LPRINT:LPRINT:LPRINT
1560 END
1570 REM ***********************************************
1580 REM START OF SUBROUTINE FOR MJ CALCULATION
1590 REM ***********************************************
1600 RHOI = RHOJ * (1 + (MSOLID / (MTAIR - MJ)))
1610 MT = MTAIR + MSOLID
1620 ALPHA = .5 * TCOEFF * (AT / AI) ^ 2 / RHOI
1630 A = ALPHA - GAMMA
1640 B = -2 * ALPHA * MT
```

```
1650 C = MT ^ 2 * (ALPHA + BETA) + THETA
1660 CHK = B ^ 2 – 4 * A * C
1670 IF CHK <= 0 GOTO 1700
1680 MJNEW = (-B – SQR(B ^ 2 – 4 * A * C)) / (2 * A)
1690 REM MJNEW1=(-B-SQRT(B ^ 2-4*A*C))/(2*A)
1700 REM
1710 RETURN
1720 REM ******************************************************
1730 REM **** CALCULATION OF FANNING FRICTION FACTOR
1740 REM ******************************************************
1750 ACOUNT = 0
1760 FFF = .025
1770 ACONST = .434294 * 4
1780 ATEMP = EXP(-1 / (ACONST * FFF ^ .5))
1790 IF RE < 3000 THE RE = 3000
1800 FF = FFF ^ .5 * ATEMP – FFF ^ .5 * ROUGH / 3.7 – 1.256 / RE
1810 FDF = .5 * FFF ^ (-.5) * (ATEMP * (1 + FFF ^ (-.5) / ACONST) – .5 * ROUGH /
3.7)
1820 AFNEW = FFF – (FF / FDF)
1830 ADIFF = ((AFNEW – FFF) / FFF) * 100
1840 FFF = AFNEW
1850 ACOUNT = ACOUNT + 1
1860 PRINT "ACOUNT="; ACOUNT
1870 PRINT "COUNT="; COUNT
1880 IF ABS(ADIFF) >= .01 THEN GOTO 1780
1890 RETURN
1900 REM ******************************************************
1910 REM **** CALCULATION OF DIFFUSER ANGLE COEFFICIENT
1920 REM ******************************************************
1930 CONTROL = 1
1940 INPUT "ENTER DIAMETER AT END OF DIFFUSER (mm) ", DF
1950 IF DF < DT THEN GOTO 1960 ELSE GOTO 1980
1960 PRINT "DIFFUSER DIAMETER IS SMALLER THAN TOTAL FLOW TUBE
DIAMETER, PLEASE TRY AGAIN"
1970 PRINT : GOTO 1940
1980 INPUT "ENTER DUFFUSER ANGLE (BETWEEN 3 & 90 DEGREES) ",
ANG1
1990 IF ANG <3 THEN GOTO 2020
2000 IF ANG1 > 90 THEN GOTO 2020 ELSE GOTO 2030
2010 PRINT
2020 PRINT "VALUE OUT OF RANGE PLEASE TRY AGAIN": PRINT : GOTO
1980
2030 IF ANG1 >= 3 THEN ZETA = -.02 * ANG1 + .24
2040 IF ANG1 >= 5 THEN ZETA = .14
2050 IF ANG1 >= 8 THEN ZETA = .01 * ANG1 + .06
2060 IF ANG1 >= 10 THEN ZETA = .0225 * ANG1 – .065
2070 IF ANG1 >= 14 THEN ZETA = .03333 * ANG1 – .21667
2080 IF ANG1 >= 20 THEN ZETA = .025 * ANG1 – .05
2090 IF ANG1 >= 30 THEN ZETA = .01667 * ANG1 + .2
2100 IF ANG1 >= 45 THEN ZETA = .01 * ANG1 + .5
2110 IF ANG1 >= 60 THEN ZETA = -.00333 * ANG1 + 1.3
2120 RETURN 180
```

APPENDIX 5 PROGRAM FOR OPTIMIZED INJECTOR JET DIAMETER

```
10 CLS
20 PRINT " ––––––––– INPUT BASIC DATA –––––––––"
30 PRINT
40 INPUT "INJECTED FLUID TUBE DIAMETER (mm) ", DI
```

```
50 INPUT "INJECTED FLUID TUBE LENGTH (m) ", LI
60 PRINT
70 INPUT "ENTER TOTAL AIR FLOW RATE (kg/h) ", MTAIRH
80 INPUT "LENGTH OF TOTAL FLOW TUBE (m) ", LT
90 PRINT
100 INPUT "ENTER SAWDUST FEED RATE (kg/h) ", SOLIDH
110 PRINT
120 INPUT "ENTER STATIC BACK PRESSURE ON INJECTOR (Pa) ", PF
130 PRINT
140 INPUT "DOES INJECTOR HAVE A DIFFUSER (Y/N) ", Q1$
150 IF Q1$ = "Y" THEN GOTO 170
160 IF Q1$ = "y" THEN GOTO 170 ELSE GOTO 180
170 GOSUB 1360
180 CONTROL = 0
190 PRINT
200 INPUT "ENTER STARTING DIAMETER FOR TOTAL FLOW TUBE (mm) ",
DT
210 REM - - - - - - - - - - - - - CONSTANTS - - - - - - - - - - - - -
220 VISCO = 1.845E-05
230 PI = 3.1415927#
240 RHOAIR = 1.2
250 REM -- Injected fluid velocity set at 8 m/s
260 VI = 8
270 SOLID = SOLIDH / 3600
280 REM - - - - - - - - - INJECTED FLUID PARAMETERS - - - - - - - - -
290 DIA = DI / 1000
300 AI = PI * (DIA / 2) ^ 2
308 CJ = .95
310 ROUGHI = .0457 / DI
320 MIAIR = VI * RHOAIR * AI
330 MI = SOLID + MIAIR
340 MIH = MIAIR * 3600
350 RHOI = RHOAIR * (1 + (SOLID / MIAIR))
360 REI = RHOI * VI * DIA / VISCO
370 ROUGH = ROUGHI
380 RE = REI
390 GOSUB 1220
400 FFFI = F
410 REM                          LOSS COEFFICIENTS
420 ENTLOSSI = .5
430 VELHEADI = 1
440 FLOSSI = 4 * FFFI * LI / DIA
450 TCOEFFI = ENTLOSSI + VELHEADI + FLOSSI
460 PLOSSI = -TCOEFFI * .5 * RHOI * VI ^ 2
470 REM - - - - - - - - TOTAL FLOW TUBE PARAMETERS - - - - - - - -
480 MTAIR = MTAIRH / 3600
490 MT = MTAIR + SOLID
500 RHOT = RHOAIR * (1 + (SOLID / MTAIR))
510 REM -- Injector exit velocity set at 16 m/s
520 IF CONTROL = 1 THEN VT = 16
530 IF CONTROL = 1 THEN AF = MTAIR / (RHOAIR * VT)
540 IF CONTROL = 1 THEN DFA = (4 * AF / PI) ^ .5
550 IF CONTROL = 1 THEN DF = DFA * 1000
560 IF CONTROL = 0 THEN DF = DT
570 LPRINT TAB(3); "- - - - - - - - - - - - - - - - - - - - - - - - - - -"
580 LPRINT TAB(7); "DT"; TAB(17); "DJ"; TAB(29); "JETPOWER"; TAB(45);
"JET TOTAL"; TAB(64); "PT"
590 LPRINT TAB(7); "mm"; TAB(17); "mm"; TAB(32); "W"; TAB(43); "PRES-
SURE (Pa)"; TAB(64); "Pa"
600 LPRINT TAB(3); "- - - - - - - - - - - - - - - - - - - - - - - - - - -"
610 REM - - - - - - - - - - - - START OF LOOP - - - - - - - - - - - -
```

```
620 DTMAX = DF
630 DTMIN = DTMAX / 4
640 FOR DT = DTMAX TO DTMIN STEP -2
650 DTA = DT / 1000
660 AT = PI * (DTA / 2) ^ 2
670 VT = MT / (RHOT * AT)
680 ROUGHT = .0457 / DT
690 RET = RHOT * VT * DTA / VISCO
700 RE = RET
710 ROUGH = ROUGHT
720 GOSUB 1220
730 FFFT = F
740 S12 = 4 * FFFT * LT / DTA
750 IF CONTROL = 0 THEN AF = AT
760 PTEMP1 = (AT / AF)
770 PTEMP2 = (MTAIR + SOLID) ^ 2 / (2 * RHOT * AT ^ 2)
780 PTEMP3 = (AT / AF) ^ 2
790 PTEMP4 = ZETA * (PTEMP1 – 1) ^ 2
800 PT = PF + CONTROL * PTEMP2 * (PTEMP4 + PTEMP3 – 1)
810 REM
820 REM – – – – – – – – – – – – JET PARAMETERS – – – – – – – – – – –
840 RHOJ = RHOAIR
850 MJ = MT – MI
860 MJH = MJ * 3600
870 TEMP1 = S12 * MT ^ 2 / (2 * RHOT * AT ^ 2)
880 TEMP2 = MT ^ 2 / (RHOT * AT)
890 TEMP3 = 1 / (RHOJ * CJ)
900 AJ = (MJ ^ 2 / (((PT – PLOSSI) + TEMP1) * AT + TEMP2)) * TEMP3
910 DJA = (4 * AJ / PI) ^ .5
920 DJ = DJA * 1000
930 VJ = MJ / (RHOJ * AJ)
940 MJVOL = MJ / RHOJ
950 MJPRESS = PLOSSI + .5 * RHOJ * VJ ^ 2
960 JPOWER = MJPRESS * MJVOL
970 REM  – – – – – – – – – – – – OUTPUT  – – – – – – – – – – – –
980 DT = INT(DT + .5)
990 DJ = INT(DJ + .5)
1000 JPOWER = INT(JPOWER + .5)
1010 MJPRESS = INT(MJPRESS + .5)
1020 PT = INT(PT + .5)
1030 MJH = INT(MJH + .5)
1040 MIH = INT(MIH + .5)
1050 LPRINT TAB(6); USING "####"; DT;
1060 LPRINT TAB(15); USING "####"; DJ;
1070 LPRINT TAB(30); USING "######"; JPOWER;
1080 LPRINT TAB(45); USING "######"; MJPRESS;
1090 LPRINT TAB(60); USING "######"; PT
1100 NEXT DT
1110 LPRINT : LPRINT
1120 LPRINT "DIAMETER OF THE INJECTED FLUID TUBE ="; DI; " mm"
1130 LPRINT "LENGTH OF TOTAL FLOW TUBE ="; LT; " m"
1140 LPRINT "LENGTH OF INJECTED FLUID TUBE ="; LI; " m"
1150 IF CONTROL = 1 THEN LPRINT "DIFFUSER ANGLE ="; ANG1; "
DEGREES"
1160 LPRINT
1170 LPRINT "TOTAL FLOW TUBE MASS FLOW RATE ="; MTAIRH; " kg/h"
1180 LPRINT "JET FLUID MASS FLOW RATE ="; MJH; " kg/h"
1190 LPRINT "INJECTED FLUID TUBE MASS FLOW RATE ="; MIH; " kg/h"
1200 LPRINT "SOLIDS MASS FLOW RATE ="; SOLIDH; " kg/h"
1210 END
1220 REM  – – – – – – CALCULATION OF FANNING FRICTION FACTOR
```

```
1230 F = .0001
1240 TEMPRE = 1.256 / RE
1250 TEMPED = ROUGH / 3.7
1260 ACONST = 4 / LOG(10)
1270 TEMP = TEMPED + TEMPRE * (F ^ -.5)
1280 FF = ((F ^ -.5) / ACONST) + LOG(TEMP)
1290 FDF = -.5 * (F ^ -1.5) * ((1 / ACONST) + (1 / TEMP) * TEMPRE)
1300 NEWF = F – FF / FDF
1310 DIFF = 100 * ABS((NEWF – F) / NEWF)
1320 F = NEWF
1330 IF DIFF >0.001 THEN GOTO 1270
1340 RETURN
1350 REM
1360 REM  – – – – – CALCULATION OF DIFFUSER ANGLE COEFFICIENT
1370 CONTROL = 1
1380 PRINT
1390 INPUT "ENTER DIFFUSER ANGLE (BETWEEN 3 & 90 DEGREES) ", ANG1
1400 IF ANG1 >= 3 THEN ZETA = -.02 * ANG1 + .24
1410 IF ANG1 >= 5 THEN ZETA = .14
1420 IF ANG1 >= 8 THEN ZETA = .01 * ANG1 + .06
1430 IF ANG1 >= 10 THEN ZETA = .0225 * ANG1 – .065
1440 IF ANG1 >= 14 THEN ZETA = .03333 * ANG1 – .21667
1450 IF ANG1 >= 20 THEN ZETA = .025 * ANG1 – .05
1460 IF ANG1 >= 30 THEN ZETA = .01667 * ANG1 + .2
1470 IF ANG1 >= 45 THEN ZETA = .01 * ANG1 + .5
1480 IF ANG1 >= 60 THEN ZETA = -.00333 * ANG1 + 1.3
1490 RETURN 210
```

Printed by Hobbs the Printers of Southampton

The Bulletin series presents the results of research and practical scientific work carried out by the Natural Resources Institute. It covers a wide spectrum of topics relevant to development issues ranging from land use assessment, through agricultural production and protection, to storage and processing.

Each Bulletin presents a detailed synthesis of the results and conclusions within one specialized area, and will be of particular relevance to colleagues within that field and others working on sustainable resource management in developing countries.

In developing countries large quantities of residues are generated when cereal, wood and oilseeds are processed.These residues are often treated as waste although they are potentially a source of energy. If converted efficiently these biomass materials could be exploited economically and could help to alleviate local environmental problems.

The **Application of Air Injectors to Biomass Combustion Systems** develops theoretical procedures for injector design and performance prediction for clean gases, and also for the entrainment of particulate materials in injectors.

The experimental use of low-pressure air injectors in the conveyance of rice husks and other particulate biomass materials in small-to-medium scale combustion systems is described and consequently this work will be of use by engineers interested in developing efficient combustion systems.